HHS Public Access

Author manuscript

Cell Stem Cell. Author manuscript; available in PMC 2019 May 03.

Published in final edited form as:

Cell Stem Cell. 2018 May 03; 22(5): 653–667.e5. doi:10.1016/j.stem.2018.03.017.

Submucosal Gland Myoepithelial Cells Are Reserve Stem Cells That Can Regenerate Mouse Tracheal Epithelium

Thomas J. Lynch[1,†], **Preston J. Anderson**[1,†], **Pavana G. Rotti**[1], **Scott R. Tyler**[1], **Adrianne K. Crooke**[1], **Soon H. Choi**[1], **Daniel T. Montoro**[5], **Carolyn L. Silverman**[1], **Weam Shahin**[1], **Rui Zhao**[5], **Chandler Jensen-Cody**[1], **Andrea Adamcakova-Dodd**[3], **T. Idil Apak Evans**[1], **Weiliang Xie**[1], **Yulong Zhang**[1], **Hongmei Mou**[5], **B. Paul Herring**[4], **Peter S. Thorne**[3], **Jayaraj Rajagopal**[5], **Charles Yeaman**[1], **Kalpaj R. Parekh**[2], and **John F. Engelhardt**[1,*]

[1]Department of Anatomy & Cell Biology, University of Iowa, Iowa City, IA 52242

[2]Department of Cardiothoracic Surgery, University of Iowa, Iowa City, IA 52242

[3]Department of Occupational and Environmental Health, University of Iowa, Iowa City, IA 52242

[4]Department of Cellular and Integrative Physiology, Indiana University, Indianapolis, IN 46202

[5]Center for Regenerative Medicine, Massachusetts General Hospital, Boston, MA 02114

Summary

The mouse trachea is thought to contain two distinct stem cell compartments that contribute to airway repair—basal cells in the surface airway epithelium (SAE) and an unknown submucosal gland (SMG) cell type. Whether a lineage relationship exists between these two stem cell compartments remains unclear. Using lineage tracing of glandular myoepithelial cells (MECs), we demonstrate that MECs can give rise to seven cell types of the SAE and SMGs following severe airway injury. MECs progressively adopted a basal cell phenotype on the SAE and established lasting progenitors capable of further regeneration following reinjury. MECs activate Wnt-regulated transcription factors (Lef-1/TCF7) following injury and Lef-1 induction in cultured MECs promoted transition to a basal cell phenotype. Surprisingly, dose-dependent MEC conditional activation of Lef-1 in vivo promoted self-limited airway regeneration in the absence of injury. Thus, modulating the Lef-1 transcriptional program in MEC-derived progenitors may have regenerative medicine applications for lung diseases.

[*]Lead Contact: John F. Engelhardt, Ph.D., Room 1-111 BSB, Department of Anatomy and Cell Biology, University of Iowa, 51 Newton Road, Iowa City, Iowa 52242, Phone: 319-335-7744, Fax: 319-335-7198, john-engelhardt@uiowa.edu.
[†]Authors contributed equally to this manuscript.

Author Contributions

Conceptualization: TL, PA, JE; Methodology: TL, JE; Analyses, TL, PA, PR, IE, ST; Investigation: TL, PA, AC, ST, SC, WX, YZ, DM, HM, WS, CS, AD, RZ; Resources: BH; Writing Original Draft: TL, JE; Writing Review & Editing: TL, PA, JR, DM, PT, CY, JE; Visualization: TL, PA, JE; Supervision: JE, J.R., PT, CY, and KP; Project Administration: TL, PA, and JE.

Competing Interests

The authors declare that there is no competing interest.

eTOC Blurb

Following severe injury to the surface airway epithelium (SAE), Wnt-signals activate myoepithelial cells in the submucosal glands (SMGs) to function as reserve stem cells for multipotent basal cells in the SAE and other SMG cell types. Lef-1 activation induces the myoepithelial cell regenerative response and a basal cell-like phenotype.

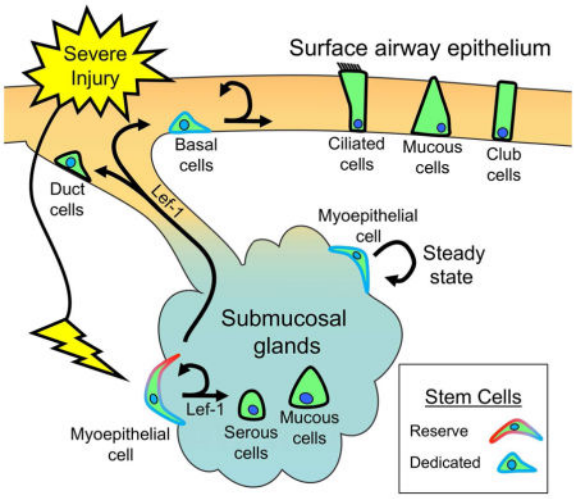

Introduction

Tissue-specific stem cells (SCs) remain one of the greatest frontiers in biomedical science and regenerative medicine. However, processes that regulate SC self-renewal, survival, and differentiation are not uniformly understood in different organs. Epithelial tissues that are exposed to the external environment, such as those of the lung, intestine, and skin, often demonstrate an incredible capacity to regenerate following injury (Hogan et al., 2014; Rajagopal and Stanger, 2016; Tetteh et al., 2015). However, limitation persist in our understanding of how epithelial SCs respond to injury and how repair after injury may differ from cellular renewal at steady state homeostasis.

Lineage-tracing studies in the mouse suggest that multiple region-specific progenitors contribute to regenerative plasticity of the airway epithelia (Hogan et al., 2014). In the trachea, extensive evidence has demonstrated that basal cells are dedicated SCs for the pseudostratified columnar epithelium under most conditions including homeostasis (Ghosh et al., 2011; Hogan et al., 2014). However, in organs with little homeostatic turnover, such as the lung, evidence has suggested that some SC niches are mobilized only after severe injury (Giangreco et al., 2009; Zacharias et al., 2018). Such findings emphasize the flexibility of SCs and their niches in responding to diverse environmental insults. In addition, the mouse trachea also contains epithelial submucosal glands (SMGs), which can also act as a regenerative SC niche for the SAE (Hegab et al., 2011; Lynch et al., 2016; Lynch and Engelhardt, 2014; Xie et al., 2011).

SMGs are grape-like tubuloacinar structures embedded within the mesenchyme beneath the SAE of all cartilaginous airways in humans and the proximal trachea of mice. Four major

anatomical domains—specified by their morphology—define SMGs: ciliated ducts, collecting ducts, mucous tubules and serous acini (Liu et al., 2004). Ciliated ducts are generally considered to be an extension of the SAE and contain similar cell types: basal, ciliated, and secretory cells. Collecting ducts, which are more extensive in larger mammals than in mice, are composed of a poorly defined simple columnar epithelium. Mucous tubules and serous acini comprise the most distal components of the glands. Finally, contractile myoepithelial cells line the collecting ducts, mucous tubules, and serous acini, but are absent in ciliated ducts. Together, these cellular compartments control the secretion of proteins and mucus important in airway innate immunity.

Progenitors have been shown to reside within gland ducts (Hegab et al., 2011). However, slowly cycling glandular progenitors that retain multiple nucleotide labels following repeated injury also reside deeper within the tubular network of SMGs (Lynch et al., 2016; Lynch and Engelhardt, 2014; Xie et al., 2011). Focal regions of high Wnt-signaling appear to be an integral component of the SMG SC niche, as label-retaining cells exist in these niches (Lynch et al., 2016). Wnt-signaling also plays an important role in establishing the glandular SC niche during post-natal development of the mouse trachea (Lynch and Engelhardt, 2014). During SMG morphogenesis, myoepithelial cells (MECs) are born early during the elongation phase as tubules invade the lamina propria and these progenitors have the capacity to differentiate into other glandular cell types but do not contribute to the SAE (Anderson et al., 2017). Thus, glandular MECs may be a resident SC for adult SMG regeneration, but this has not been formally tested.

Tracheal SMGs might serve as a protected SC niche, sequestering epithelial SCs from the more exposed environment of the SAE (Lynch and Engelhardt, 2014). We therefore hypothesized that, following severe injury, reserve SCs located deep within the SMGs are able to regenerate the SAE. In this context, we define “reserve SCs” as multipotent cells capable of imparting a regenerative response in the setting of a specific type or severity of injury and giving rise to dedicated SCs. Herein we refer to “dedicated SCs” as multipotent progenitors that are the primary source of cellular regeneration for a tissue under most conditions. Using lineage tracing, we demonstrate that glandular MECs are multipotent progenitors of both SAE and SMG cell types following severe injury. Furthermore, we demonstrate that the Wnt-signaling transcription factor, Lef-1, is sufficient to activate lineage commitment of MECs and their regenerative responses. We define “MEC lineage commitment” as a process whereby MECs exit their endogenous niche and assume an altered progenitor cell phenotype capable of multipotent differentiation. Given that humans possess SMGs throughout the cartilaginous airways, this SC niche may play a significant role in lung regeneration and disease.

Results

αSMA$^+$ epithelial cells emerge on the airway surface after severe but not moderate injury

We hypothesized that the extent of injury to the SAE is a determinant of whether reserve progenitors residing deep within the SMGs are mobilized for airway repair. To test this, we evaluated the proliferative responses of cells in the SAE and SMGs following moderate (200 mg/kg naphthalene) and severe (300 mg/kg naphthalene) epithelial injury. As hypothesized,

severe injury increased EdU incorporation (2 hr pulse) within the SMG epithelium to a significantly greater extent than moderate injury (8.6-fold, $P<0.0001$, N=3–6 mice) at 3 days post-injury (DPI). Interestingly, αSMA$^+$ epithelial cells emerged on the SAE only following severe injury, peaking at 3 DPI (Figure S1A–D) and coinciding with a 2.7-fold increase in the number of αSMA$^+$ MECs in the SMGs as compared to moderate injury (Figure S1E). Given that the only αSMA-expressing epithelial cells in this region of the trachea are glandular MECs, these findings suggested that glandular MECs might transiently expand following severe injury and migrate to the SAE to facilitate repair.

Glandular MECs have the capacity to repair the tracheal SAE following severe naphthalene injury

To determine if glandular MECs contribute to repair of the tracheal SAE following severe injury, we evaluated the suitability of two Cre drivers for lineage-tracing, which were predicted to mark MECs based on expression of αSMA/*ACTA2* (alpha smooth muscle actin-2) or SMMHC/*MYH11* (smooth muscle myosin heavy chain or myosin heavy chain 11). We crossed these Cre drivers to a ROSA^{LoxP}tdTomato^{StopLoxP}EGFP Cre reporter (ROSA-TG), to obtain *ACTA2*-Cre^{ERT2}:ROSA-TG and *MYH11*-Cre^{ERT2}:ROSA-TG mice. Tamoxifen induction with either *ACTA2*-Cre^{ERT2} or *MYH11*-Cre^{ERT2} resulted in a MEC labeling efficiency of 77% and 85%, respectively (Figure S1F–J). Thus, both Cre drivers appeared suitable for lineage tracing MECs following injury.

To test the hypothesis that MECs contribute to airway repair following severe injury, we injured lineage-traced *ACTA2*-Cre^{ERT2}:ROSA-TG mice with vehicle or high dose naphthalene (300 mg/kg) and examined the distribution of traced cells at 14 or 21 days post-injury (DPI) (Figure 1A). At 14 DPI, lineage-traced (GFP$^+$) cells emerged on the SAE and assumed a basal cell-like morphology (Figure 1B–C). Interestingly, traced cells in the proximal tracheal SAE retained αSMA expression, whereas more distal GFP$^+$ cells lacked αSMA expression (Figure 1B). Traced cells on the SAE adopted a basal cell phenotype, expressing cytokeratin 5 (Krt5) (Figure 1C), Krt14 (Figure 1H), and neural growth factor receptor (NGFR) (Figure 1E,F). Notably, both NGFR$^+$ and NGFR$^-$ traced basal-like cells on the SAE were observed (Figure 1E,F), suggesting that MECs adopt an NGFR$^+$ phenotype on the airway surface. Traced cells expressing tumor-associated calcium signal transducer 2 (Trop2), which specifically marks SAE and SMG duct progenitors (Hegab et al., 2011), were also observed in gland ducts (Figure 1D). By 21 DPI, infrequent traced Krt8$^+$ columnar cells appeared in the SAE (Figure 1G), an indication of basal cell differentiation. In the absence of injury, traced SAE cells were not observed in the SAE (Figure 1I).

These findings suggest that MEC-derived progenitors on the SAE progressively extinguish αSMA expression while adopting a basal cell phenotype (Krt5$^+$Krt14$^+$NGFR$^+$) with the ability to differentiate into Krt8$^+$ luminal columnar cells. We thus quantified the percentage and phenotype of traced cells along the proximodistal axis of the tracheal SAE at 21 DPI (Figure 1J–L). Traced cells accounted for ~14% of the SAE between the cricoid cartilage (C0) and cartilage ring 4 (C4) (Figure 1J), with the highest percentage in the C0–C1 region and 2–3 fold lower levels further from the glands at C2–C4 (Figure 1K). This later finding supports the notion that MEC-derived progenitors emerge from the most proximal and

largest glands in the C0–C1 region and migrate distally. Interestingly, the percentage of GFP$^+$αSMA$^+$ traced cells declined along the C0–C4 proximodistal axis of the trachea, while the percentage of GFP$^+$Krt8$^+$ demonstrated the opposite trend (Figure 1L). Despite the observed heterogeneity of NGFR expression in traced SAE basal-like cells, there was no proximodistal axis pattern of expression following quantification. Cumulatively, these findings demonstrate several important features regarding MEC-derived progenitors on the airway surface: 1) MEC contribution to the SAE is maximal above the most proximal tracheal gland; 2) MEC-derived progenitors in the SAE adopt a basal cell phenotype as they move distally down the trachea by extinguishing αSMA expression and increasing their ability to differentiate into Krt8$^+$ columnar cells; and 3) the vast majority of lineage-traced MECs remain in an undifferentiated basal-like state at 21 DPI.

The use of lineage-restricted Cre-drivers for fate mapping comes with caveats that include both the specificity of the promoters used and lineage tracing efficiency (Rios et al., 2016). Thus, we sought to validate our findings using *MYH11*-Cre^{ERT2} lineage tracing, which also efficiently marks MECs in adult SMGs (Figure S1G–J). Similarly to *ACTA2*-Cre^{ERT2}:ROSA-TG mice, naphthalene injury of *MYH11*-Cre^{ERT2}:ROSA-TG mice also led to the appearance of Krt5 and Krt14 lineage-traced basal cells in the SAE (Figure S2A–C,F). Furthermore, extending the chase period following tamoxifen induction from 5 to 21 days did not alter MEC contribution to SAE repair following naphthalene injury of *ACTA2*-Cre^{ERT2}:ROSA-TG mice (data not shown).

Glandular MEC-derived basal cells in the SAE have the capacity to differentiate into ciliated cells

We next examined the potential of MEC-derived progenitors to expand over time in the SAE and generate ciliated cells following severe naphthalene injury of *ACTA2*-Cre^{ERT2}:ROSA-TG mice (Figure 2A). The percentage of traced cells in the SAE rose 4.5-fold between 7 and 60 DPI (Figure 2J), suggesting that MEC progenitors expand within the SAE over time. Similarly, traced acetylated αtubulin$^+$ ciliated cells also increased ~4-fold during this time frame (Figure 2C–I,K), confirming that MEC-derived basal cells take time to mature and differentiate. Naphthalene injury of *MYH11*-Cre^{ERT2}:ROSA-TG mice also produced infrequent ciliated cells at 21 DPI (Figure S2E). In the absence of injury, traced MECs failed to migrate to the SAE even after a 1.5 year chase (Figure 2L), demonstrating that MEC-derived progenitors do not participate in maintaining homeostatic turnover of the SAE. Taken together, these data demonstrate that MEC-derived progenitors can contribute to repair of the SAE following severe injury by adopting a basal cell phenotype and differentiating with time.

MEC-derived basal cells establish long-lasting residence in the SAE capable of further expansion following reinjury

Our findings suggest that MEC-derived progenitors on the SAE remain relatively undifferentiated at 21 DPI, but with increasing time after injury can differentiate into ciliated cells. However, it remained unclear if traced basal cells in the SAE indeed reestablished multipotent SC niches capable of responding to a second injury. To address this question, we performed repeated epithelial injury on tamoxifen-induced *ACTA2*-Cre^{ERT2}:ROSA-TG

mice using first, a severe injury that largely ablates SAE basal cells, followed by a moderate injury that applies regenerative pressure to primarily SAE basal cells (Figure 3A). Following this sequential injury, large lineage-traced clone-like patches on the airway surface contained multiple cell types typical of the SAE (Figure 3B), including αtubulin$^+$ ciliated cells, non-ciliated columnar cells (Figure 3C), and goblet cells marked by *Ulex europaeus* agglutinin I (UEA-1) [lectin with specific affinity for Muc5AC (Pardo-Saganta et al., 2013)] (Figure 3H), and Muc5B (Figure 3I). Notably, while traced Scgb1a1$^+$ club cells were rarely observed, a second injury led to the appearance of traced Scgb3a2$^+$ club cells (Figure 3D,K).

We quantified the abundance of traced cells in the SAE of *ACTA2*-Cre^{ERT2}:ROSA-TG mice after a single injury (SI) or double injury (DI) protocol as compared to uninduced (UNIND) and uninjured (UI) control mice. At 60 DPI, there was a 1.6-fold increase in the percentage of traced cells following double injury as compared to a single injury (Figure 3L). This demonstrates that MEC-derived progenitors in the SAE are capable of further expansion following reinjury. By quantifying the distribution of ciliated, club, and goblet cells in the native (untraced/Tomato$^+$) and MEC-derived (lineage-traced/GFP$^+$) SAE of the same samples, we asked whether MEC-derived progenitors adopt a similar multipotency as resident SAE progenitors (Figure 3N). Following a single injury, MEC-derived progenitors retained a bias toward differentiating into Muc5B$^+$ goblet cells and ciliated cells, while in the native untraced epithelium Scgb3a2$^+$ and Scgb1a1$^+$ club cells and ciliated cells were the predominant secretory cell types (Figure 3N). Interestingly, a second injury partially reversed this secretory cell bias leading to fewer traced Muc5B$^+$ goblet cells (2.6-fold) and greater numbers of Scgb3a2$^+$ club cells (10-fold). Taken together, these findings suggest that the differentiation potential of MEC-derived basal cells is not equivalent to that of SAE basal cells. However, with time and pressure to expand, MEC-derived basal cells appear to converge on a more native basal cell phenotype.

Glandular MECs have the capacity to differentiate into other glandular cell types following airway injury

ACTA2-Cre^{ERT2}:ROSA-TG labeled MECs were also capable of generating mucus secreting glandular tubules marked by UEA-1 (Figure 3G) and Muc5B (Figure 3I,J), as well as serous cells marked by lysozyme (Figure 3F) and DBA (Figure 3E). Following a single injury, traced cells in the SMGs doubled (Figure 3M). As expected, the percentage of traced cells in the SMGs did not increase following a second mild injury, since this level of injury does not lead to MEC expansion. However, a second injury led to a decline in traced Trop2$^+$ duct cells (~3-fold) and a rise in Muc5B$^+$ (~3-fold) and UEA-1$^+$ (~10-fold) glandular cells (Figure 3O). The decline in traced Trop2$^+$ duct cells is consistent with gland ducts serving as a reservoir for SAE basal cells following moderate injury without selective pressure for repopulating this niche from glandular MECs. MEC lineage contribution to SMG tubules and ducts was also observed in *MYH11*-Cre^{ERT2}:ROSA-TG mice following a single severe naphthalene injury (Figure S2B,D). These data demonstrate that MECs also can differentiate into other glandular cell types.

Glandular MEC progenitors participate in airway repair following SO_2 injury

In multiple organs, the type of insult and extent of injury can influence the type of stem cells that participate in epithelial regeneration (Hogan et al., 2014). This feature of stem cell plasticity is vital to the homeostatic maintenance and repair of organs in the face of diverse environmental insults. To determine if MEC-mediated repair of tracheal SAE and SMGs was specific to naphthalene injury, we performed lineage-tracing experiments in *ACTA2*-Cre^{ERT2}:ROSA-TG mice injured with SO_2 three weeks following tamoxifen induction (Figure S3A). SO_2 injury has been used to rapidly ablate luminal cells in the trachea leading to a basal cell regenerative response (Tadokoro et al., 2016). Similar to naphthalene injury, mice exposed to SO_2 rapidly mobilized lineage-traced MECs to the SAE where they adopted a basal cell phenotype (Figure S3B–G,K). Furthermore, lineage-traced glandular tubules emerged with time post-SO_2 injury (Figure S3H–J,L). MEC-derived cells in the SAE extinguished αSMA expression with time post-injury as $Krt5^+$ and $Krt14^+$ basal cells expanded and differentiated into $Krt8^+$ luminal cells (Figure S3M). These studies demonstrate that MECs can also function as progenitors of SAE basal cells following SO_2 airway injury.

The Wnt-regulated program of primordial glandular stem cells is adopted by MECs following airway injury

Developmental programs that regulate stem cells during organ morphogenesis are often repurposed for regulating stem cell regenerative responses in adult tissues (Clevers et al., 2014; Lynch and Engelhardt, 2014; Tata and Rajagopal, 2017). During the earliest stages of SMG morphogenesis, Wnt-mediated transcriptional activation of lymphoid enhancer factor 1 (*Lef-1*) is required for primordial glandular stems cells (PGSCs) to initiate gland development from placodes in the SAE (Duan et al., 1999). Repression of SRY-Box 2 (Sox2) within PGSCs acts in concert with Wnt/β-Catenin signals to activate transcription at the *Lef-1* promoter (Driskell et al., 2004; Filali et al., 2002; Liu et al., 2010; Lynch et al., 2016; Xie et al., 2014). In the absence of *Lef-1*, PGSCs fail to proliferate and gland development is aborted at an early stage of elongation (Driskell et al., 2007). We discovered that Transcription Factor 7 (TCF7) is also activated within PGSCs in a similar fashion to Lef-1 (Figure 4A,B). We hypothesized that these transcription factors may be similarly regulated during lineage commitment of adult MECs following airway injury.

To this end, we evaluated the nuclear expression profiles of Lef-1, TCF7, Sox2, and β-Catenin in SMGs at 12 and 24 hrs following naphthalene injury (Figure 4C–L). In the uninjured state, Sox2 was expressed in the majority of SMG cells and $αSMA^+$ MECs, but Lef-1 and TCF7 expression was largely absent (Figure 4C–E,K,L); nuclear β-Catenin expression was largely confined to glandular cells that did not express the MEC marker αSMA (Figure 4F,K,L). By contrast, airway injury with naphthalene induced nuclear Lef-1, TCF7, and β-Catenin in a large proportion of MECs by 24 hrs, while Sox2 expression was largely extinguished in MECs and other glandular cell types (Figure 4G–L). By 5 DPI Lef-1 expression declined toward basal levels, and Sox2 expression increased back to uninjured levels (data not shown). Thus, injury induced changes in the expression of these transcription factors and nuclear β-Catenin within MECs appear conserved with the pattern seen in PGSCs during early stages of gland development.

Lef-1 expression within glandular MECs activates lineage commitment and a regenerative response

Given that Lef-1 is required for lineage commitment of PGSCs during gland development and is also activated in MECs shortly after airway injury, we hypothesized that this transcription factor may also control lineage commitment of MECs following injury. To test this hypothesis, we utilized a ROSA^{LoxP}EGFP^{StopLoxP}Lef-1 (Lef-1KI) knock-in transgene capable of lineage-tracing cells that activate Lef-1 expression in response to Cre (Figure 5A). We first asked if induction of Lef-1 expression in MECs over a 5 day time course leads to replication of MECs as detected by EdU incorporation (Figure 5B). Surprisingly, tamoxifen induction of *ACTA2*-Cre^{ERT2}:Lef-1KI$^{+/+}$ mice (homozygous for the Lef-1KI transgene) led to significant expansion of lineage-traced cells (GFP^{-}) in the SMG and SAE, as compared to uninduced controls (Figure 5C,E). Furthermore, traced regions of Lef-1KI$^{+/+}$ SMGs contained more replicating MECs (i.e., EdU^{+}) compared to untraced regions (Figure 5E,F) and tamoxifen-induced uninjured *ACTA2*-Cre^{ERT2}:ROSA-TG mice (Figure 5D,F). These findings support the hypothesis that Lef-1 induction in MECs controls lineage commitment to SAE and SMG cell types. However, the lack of EdU in the majority of Lef-1KI traced cells remained somewhat puzzling and suggested that the lineage commitment process may not always require replication of MECs.

To better understand the process by which Lef-1 activation in MECs controls regenerative expansion, we evaluated uninjured and naphthalene injured *ACTA2*-Cre^{ERT2} traced mice heterozygous (Lef-1KI$^{+/-}$) and homozygous (Lef-1KI$^{+/+}$) for the Lef-1KI transgene (Figure 5G–U). Importantly, without tamoxifen induction, injured Lef-1KI$^{+/+}$ mice retained GFP expression in both SMGs and the SAE (Figure 5H). Interestingly, while induced/uninjured Lef-1KI$^{+/+}$ increased lineage-traced cells (i.e., GFP^{-}) in both the SAE and SMGs, this did not occur in induced/uninjured Lef-1KI$^{+/-}$ animals (Figure 5I,K,T,U). Following naphthalene injury, both Lef-1KI$^{+/-}$ and Lef-1KI$^{+/+}$ animals demonstrated enhanced lineage contribution to the SAE (~4–5 fold) (Figure 5J,L,U) when compared to single injury *ACTA2*-Cre^{ERT2}:ROSA-TG animals lacking the Lef-1KI transgene (Figure 1J). As anticipated, the extent of nuclear Lef-1 expression was similar to the extent of lineage-trace (i.e., GFP^{-}) in various treatment groups and Lef-1KI genotypes (Figure 5M–S), with Lef-1 expressing SAE cells also observed in the distal trachea of Lef-1KI$^{+/+}$ animals (Figure 5N,O insets). Interestingly, both traced (GFP^{-}) and untraced (GFP^{+}) cells expressed Sox2, and this was true in both the SAE and SMGs, suggesting that Lef-1 overexpression does not directly repress Sox2 expression (data not shown). Similar findings of enhanced regeneration of the SAE and SMGs were also observed in *MYH11*-Cre^{ERT2}:Lef-1KI$^{+/-}$ mice following naphthalene injury (Figure S4). Thus, induction of Lef-1 in MECs enhances the regenerative properties of this progenitor cell following airway injury and a high level of Lef-1 expression (i.e., Lef-1KI$^{+/+}$) is sufficient to drive lineage commitment of MECs in the absence of injury.

We next evaluated whether induction of Lef-1 in MECs altered the ability of MEC-derived progenitors to differentiate into various cell types of the SAE and SMGs. Following naphthalene injury, *ACTA2*-Cre^{ERT2}:Lef-1KI$^{+/-}$ MECs (here forward called MEC$^{Lef-1KI}$) were able to differentiate into SAE basal (Krt5^{+}), club (Scgb1a1^{+}), and ciliated (αtubulin^{+})

cells, but UEA-1^{+} secretory cells were infrequently observed (Figure 6A–F,K). Thus, the secretory cell bias for MEC^{WT} progenitors (i.e., goblet) differed from that of MEC$^{Lef\text{-}1KI}$ progenitors (i.e., club). Similarly, MEC$^{Lef\text{-}1KI}$-derived cells in the SMGs differentiated into glandular duct (Trop2^{+}), ciliated duct (αtubulin^{+}), and serous (UEA-1^{+}) cells following injury (Figure 6G–J).

Sufficient Lef-1 expression in MECs induces a self-limiting regenerative response by directional commitment without self-renewal of its SC phenotype

During mouse postnatal tracheal development, Lef-1 is specifically expressed in highly proliferative glandular progenitor cells and is extinguished as glands mature. By analogy, it is interesting that biallelic induction of Lef-1KI in adult MECs gave rise to a surprisingly robust regenerative response in the absence of injury. However, this response was not accompanied by unlimited proliferative expansion, suggesting that Lef-1 functions may be limited to glandular SC niches. We hypothesized that high levels of Lef-1 expression might induce lineage commitment of MECs in the absence of self-renewing its precursor SC state. To this end, we SO_2-injured *ACTA2*-Cre^{ERT2}:Lef-1KI$^{+/+}$ mice sequentially at 21 and 42 days post-tamoxifen induction (Figure 6L) and asked whether untraced MECs (i.e., GFP^{+}) repopulated the SMG and SAE following re-injury. Indeed, induced/uninjured Lef-1KI$^{+/+}$ animals retained large numbers of lineage-traced cells (GFP^{-}) in the SMG and SAE out to 62 days following tamoxifen induction (Figure 6M), while untraced cells (GFP^{+}) repopulated most of the SAE and SMGs in sequentially injured Lef-1KI$^{+/+}$ mice (Figure 6N–O). This finding suggests that untraced MECs, which fail to activate Lef-1, repopulate the SMGs and expand following re-injury. Thus, sufficient Lef-1 expression in multipotent MECs may activate a state of limited potential to self-renew in the SAE and SMGs.

Lef-1 expression in MECs activates pathways consistent with a regenerative response

Wnt signals play important roles in regulating stem cells and their niches in many organs (Clevers et al., 2014). To evaluate how Lef-1, a component of canonical Wnt signaling, alters the phenotype and regenerative response of MECs, we performed RNAseq on passage-1 (P1) FACS isolated lineage-traced MECs harvested from SMGs of tamoxifen induced *ACTA2*-Cre^{ERT2}:Lef-1KI$^{+/+}$ and *ACTA2*-Cre^{ERT2}:ROSA-TG mice. Of the 13,336 expressed genes identified, 699 genes had altered expression >2-fold between MEC$^{Lef\text{-}1KI}$ and MEC^{WT} populations, the majority (537 genes) being induced in MEC$^{Lef\text{-}1KI}$ (Table S1). There were 359 differentially expressed genes (Benjamini-Hochberg adjusted t-test; $P<0.05$) of which 94% were upregulated by Lef-1 (Figure 7A). Lef-1 expression was induced ~150-fold in MEC$^{Lef\text{-}1KI}$ (Figure 7B). Principle components analysis (PCA) of all 13,336 expressed genes demonstrated a clear separation of MEC^{WT} from MEC$^{Lef\text{-}1KI}$ transcriptomes with the first two PCs accounting for 64.55% of the total variance (Figure 7C). Ingenuity pathway analysis was used to discover biological pathways that were significantly differentially regulated in MEC^{WT} and MEC$^{Lef\text{-}1KI}$ transcriptomes (Figure 7D) and demonstrated positive z-scores for pathways involved in *cell movement* (Figure 7E), *migration of cells* (Figure 7F), *formation of the lung* (Figure 7H), and *branching of epithelial tissues* (Figure 7I) (Table S2). By contrast, significant negative z-scores included gene sets involved in *organismal death* (Figure 7G), *cell death,* and *apoptosis* (Figure 7D). These findings are consistent with Lef-1 activation of a transcriptional program that drives

migration of MECs to the SAE and promotes a regenerative response. In this regard, 41 transcription factors were differentially regulated in MEC^{WT} and $MEC^{Lef\text{-}1KI}$ populations (Figure 7L). For example, $MEC^{Lef\text{-}1KI}$ induced *Tbx4* (3.3-fold), which has been implicated in regulating proliferation, migration, and invasion of lung myofibroblasts (Xie et al., 2016). Two other Lef-1-induced transcription factors, *TWIST2* (3.9-fold) and *Zeb1* (3.4-fold), regulate epithelial cell adhesion, motility and proliferation (Browne et al., 2010; Teng and Li, 2014). Consistent with enhanced transcriptional pathways involved in migration, $MEC^{Lef\text{-}1KI}$ cells demonstrated enhanced motility compared to MEC^{WT} cells in culture (Figure 7J,K). How various components of the culture media (i.e., Wnt agonists, SMAD inhibitors, BMP inhibitor, TGFβ inhibitor, and ROCK inhibitor) influence these Lef-1-dependent effects remains to be determined.

Lef-1 expression facilitates lineage commitment of MECs toward a SAE basal cell phenotype

Given that Lef-1 expression in MECs led to more rapid regeneration of the SAE, we hypothesized that Lef-1 may induce MEC lineage commitment toward a SAE basal cell phenotype. To address this hypothesis, we asked whether the transcriptome of primary cultures of $MEC^{Lef\text{-}1KI}$ cells is more closely related to that of SAE basal cells than that of MEC^{WT} cells. To identify key genes that define SAE basal cells, we FACS isolated basal, ciliated, and club cell populations as previously reported (Zhao et al., 2014) and performed microarray analysis on isolated mRNA (Figure S5A). Principal component analysis (Figure S5B) and hierarchical clustering (Figure S5C) demonstrated robust differences in gene expression between basal, ciliated and club cell samples including enrichment of previously identified cell-type specific genes (e.g., basal cells: *Cdh3, Ngfr, Trp63, Notch1, Krt14, Krt5*; ciliated cells: *Cfap46, Tuba1a, Foxj1, Rfx3*; and club cells: *Aldh1a7, Cyp7b1, Notch3, Scgb3a2*) (Figure S5D)(Table S3). Of the 1215 genes enriched in basal cells (z-score >1.5; Table S3B), 50 genes were differentially regulated >2-fold between MEC^{WT} and $MEC^{Lef\text{-}1KI}$ populations and 92% of these genes were upregulated in $MEC^{Lef\text{-}1KI}$ (Figure 7M). These findings demonstrate that Lef-1 induces a phenotypic shift in MECs toward SAE basal cells, supporting the notion that Lef-1 induction in MECs following airway injury controls lineage commitment and migration to the airway surface where MECs differentiate into basal cells.

MECs are highly proliferative self-renewing progenitors

Important criteria for stemness include the ability to self-renew and maintain multipotency for differentiated cell types in a given biologic trophic unit (Lanza and Atala, 2014). The ability to demonstrate these criteria in vitro provides important support for stemness. To this end, we first sought to compare the ability of SAE basal cells and MEC^{WT} populations for their ability to self-renew in culture. We differentially isolated primary SAE and SMG cells from tamoxifen-induced *ACTA2*-Cre^{ERT2}:ROSA-TG mice and expanded them in vitro (Figure S6A–F). Traced MECs were not present among the isolated SAE cells (Figure S6B,C), but were found in SMG epithelia (Figure S6E,F). As expected from in vivo quantification, traced MECs (GFP^{+}) represented a minority of glandular cells upon initial plating (~15%), but with time expanded more extensively than did untraced glandular progenitors, stabilizing at ~75% of cultures by P5–P7 (Figure S6F). Assuming 23% of

MECs are untraced (Figure S1I,J), this stabilized ratio likely represents the outgrowth of traced and untraced MECs. However, an alternative explanation for the persistence of untraced cells could be the contamination of glandular preparations with SAE basal cells with an equal capacity for self-renewal.

To better distinguish between these two possibilities, we performed mixing experiments with FACS isolated P3 cultures of *ACTA2*-Cre^{ERT2}:ROSA-TG SMG progenitors (untraced/Tomato^{+} or traced/GFP^{+}) and transgene-negative SAE progenitors mixed at a ratio of 10%SMG:90%SAE (Figure S6G–L). In both conditions traced (GFP^{+}) and untraced (Tomato^{+}) gland-derived cells expanded to a greater extent than SAE-derived cells in mixed cultures (Figure S6I,L). Thus, it is unlikely that contaminating SAE basal cells are the untraced lineage that persists in glandular culture. Given the enhanced regenerative capacity of MEC$^{Lef\text{-}1KI}$-derived progenitors in vivo, we hypothesized that Lef-1 expression may impart a greater capacity to proliferate in vitro. To this end, we compared the ability of MEC^{WT} and MEC$^{Lef\text{-}1KI}$ populations for their ability to self-renew in mixed cultures containing 10%-MEC$^{Lef\text{-}1KI}$:90%-MEC^{WT}. Results from this analysis demonstrated that indeed MEC$^{Lef\text{-}1KI}$ outcompeted MEC^{WT} progenitors in culture (Figure S6M–O). Thus, Lef-1 expression in MECs either enhances the extent of self-renewal or reduces cell cycle time under culture conditions that promote Wnt signaling and inhibit SMAD signaling (Mou et al., 2016). Limitations to the above comparisons include the fact that the specific conditions of the culture system could impact growth and self-renewal of diverse progenitor populations differently.

MECs are multipotent progenitors for SAE cell types in vitro and rapidly regenerate a differentiated airway epithelium in denuded tracheal xenografts

To compare the capacity of MEC^{WT} and MEC$^{Lef\text{-}1KI}$ progenitors to differentiate in vitro, we mixed P1 populations (50:50) and seeded them into air-liquid interface (ALI) cultures and denuded tracheal xenografts (Figure S7A). Phenotypic analysis of ALI cultures demonstrated that MEC$^{Lef\text{-}1KI}$ more effectively generated Scgb1a1 expressing club cells (Figure S7B,F) than MEC^{WT}, supporting in vivo findings. While both MEC^{WT} and MEC$^{Lef\text{-}1KI}$ progenitors differentiated into α-tubulin expressing ciliated cells, MEC$^{Lef\text{-}1KI}$ did this to a greater extent (Figure S7C,G). Relatively few Muc5AC expressing secretory cells were observed and only in the MEC$^{Lef\text{-}1KI}$ populations (Figure S7D,H), while Muc5B expressing secretory cells were observed equally in both populations (Figure S7E,I).

We next utilized reconstituted denuded tracheal xenografts in athymic nude mice to interrogate the capacity of SAE and SMG progenitors to both proliferate and differentiate (Lynch et al., 2016), by seeding mixed population of primary cells isolated from non-transgenic tracheal SAE and *ACTA2*-Cre^{ERT2}:ROSA-TG SMGs containing traced and untraced cells at a ratio of 1:9 (SMG:SAE). Notably, both SMG lineage-traced (GFP^{+}) and untraced (Tomato^{+}) cells generated gland-like clones, whereas unmarked SAE cells rarely contributed to glands despite the seeding of 9-fold more SAE cells (Figure S7J). Traced MEC-derived progenitors also generated SAE clones containing ciliated cells (Figure S7K) and luminal mucin secreting cells (Figure S7L). Thus, in xenografts MEC-derived progenitors are capable of differentiating into both SMG and SAE cell types. Furthermore,

SMG-derived cells contributed to a larger portion of the xenograft epithelium than did SAE-derived transgene negative cells, supporting the finding that MECs have enhanced growth properties in vitro relative to SAE cells.

To directly compare the capacity of MEC^{WT} and $MEC^{Lef\text{-}1KI}$ progenitors to regenerate a denuded epithelium, we seeded xenografts with a 50:50 mixture of FACS isolated, lineage-traced, populations. Findings from these studies were similar to the in vitro expansion assays. The majority of the xenograft epithelium was reconstituted by the GFP^{-} $MEC^{Lef\text{-}1KI}$ population (Figure S7M–O). While both MEC^{WT} and $MEC^{Lef\text{-}1KI}$ progenitors formed lineage-mixed gland-like structures, a greater number were observed with the $MEC^{Lef\text{-}1KI}$ phenotype (GFP^{-}) (Figure S7M,N). Furthermore, both MEC^{WT} and $MEC^{Lef\text{-}1KI}$ progenitors had the ability to differentiate into ciliated cells (Figure S7P,Q). These ex vivo findings confirm that Lef-1 expression in MECs enhances the regenerative capacity of this stem cell, as observed both in vivo and in vitro.

Discussion

SC niches coordinate tissue maintenance and repair in adult organs and these processes often require regenerative plasticity capable of adapting to the extent and type of injury (Hogan et al., 2014; Rajagopal and Stanger, 2016). In proximal airways, two anatomically distinct SC niches are thought to exist in SAE and SMGs. While basal cells have been formally defined as SCs of the SAE using in vivo lineage-tracing and in vitro criteria, the identity of SMG SCs has remained unclear. Our findings demonstrate that glandular MECs are precursors of multipotent SAE basal SCs and other glandular cell types following severe airway injury. Given the anatomical separation of these two SC compartments and distinct biologic functions of each epithelium, we conclude that glandular MECs are reserve multipotent SCs of the SAE and are dedicated SCs of SMGs.

Glandular MECs only contributed to SAE repair following severe airway injury and did not contribute to homeostatic maintenance of the SAE over 1.5 yrs. Thus, MECs fit the criteria of a reserve SC for the SAE. Interestingly, lineage-traced MECs in the SAE progressively extinguished αSMA expression in a proximodistal pattern along the trachea as they adopted a basal cell phenotype in the SAE. This maturation process coincided with increased differentiation into luminal cells. While MEC-derived basal cells in the SAE were multipotent, forming ciliated, secretory, and non-ciliated columnar cells by 60 days following a single injury, their differentiation potential was not equivalent to that of native SAE basal cells. For example, MEC-derived $Scg3a2^{+}$ club cells only emerged following a second mild injury, and these cells lacked Scg1a1 expression typical of native club cells. Thus, while MEC-derived progenitors can establish lasting residence in the SAE and expand following a second injury, they take considerable time to mature into dedicated basal stem cells.

Mammary gland MECs have been extensively studied by fate mapping and may be analogous to airway gland MECs. Both mammary MECs and luminal cells are long-lived lineage-restricted progenitors during development, puberty, and pregnancy; yet, isolated mammary MECs, but not isolated luminal cells, can form whole mammary glands in

transplantation assays (Prater et al., 2014; Van Keymeulen et al., 2011). Similar to these studies, airway glandular MECs appear lineage-restricted in vivo in the absence of severe injury, yet only airway gland MECs, not SAE basal cells, generate both a well-differentiated surface epithelium and gland-like structures in xenograft transplantation assays. Moreover, during development a subset of mammary MECs have the capacity to differentiate into luminal cells (Rios et al., 2014). In this regard, we have similarly shown that early-born MECs are able to differentiate into multiple SMG cell types during tracheal development (Anderson et al., 2017). We now show that adult tracheal MECs are multipotent SCs for serous, mucous, and duct cells of SMGs following airway injury.

Wnt/β-catenin signaling is integral to many developmental programs involved in organogenesis and these pathways are often repurposed by SC niches to regulate regenerative responses in adult tissues (Clevers et al., 2014; Nusse and Clevers, 2017). In this regard, we find striking similarities in the dynamic expression of several Wnt-regulated transcription factors (Lef-1^{Hi}, $TCF7^{Hi}$, and $Sox2^{Low}$) during lineage commitment of primordial glandular SCs (PGSCs) (Lynch and Engelhardt, 2014) and adult glandular MECs following airway injury. Interestingly, SCs at the tips of pseudoglandular stage embryonic human airways also retain a similar expression pattern (Nikolic et al., 2017). These three types of airway SCs also likely share invasive and migratory phenotypes during development and regeneration. Our findings in MECs suggest that Lef-1 expression may drive this phenotype. Consistent with this notion, biallelic Lef-1KI expression in MECs was sufficient to activate lineage commitment and migration to the SAE in the absence of injury, while also enhancing transcriptional pathways that control migration, invasiveness and proliferation in cultured MECs. Biallelic Lef-1KI expression also shifted the MEC transcriptome toward a basal cell phenotype, which was consistent with an enhanced capacity of $MEC^{Lef\text{-}1KI}$ to differentiate into $Scgb1a1^{+}$ club cells in vivo and in vitro.

Canonical Wnt/β-catenin signaling mediated by TCF/Lef-1 family members is thought to be primarily regulated through post-transcriptional processes that control the availability of nuclear β-catenin to engage DNA-bound TCF/Lef-1 transcription factors (Nusse and Clevers, 2017). In the absence of nuclear β-catenin, enhancer-bound TCF/Lef-1 complexes are thought to repress transcription. However, PGSCs during airway gland development appear to utilize a slightly altered mode of Wnt signaling, where Wnt3a induces both transcription of *Lef-1* and levels of nuclear β-catenin (Driskell et al., 2004; Filali et al., 2002; Liu et al., 2010; Lynch et al., 2016; Xie et al., 2014). In this regard, MECs appear to behave similarly since they also induce Lef-1 expression and nuclear β-catenin following injury. Given that slowly cycling SMG SCs reside near these Wnt-active niches (Lynch et al., 2016), we hypothesize that the SMG niche responds to severe SAE injury by modulating Wnt signals that induce *Lef-1* expression, which leads to self-renewal and asymmetric production of multipotent MEC-daughter cells. The requirement for an inductive signal (i.e., Wnt stimulated nuclear β-catenin) to promote lineage commitment of MECs is consistent with the minimal contribution of MECs to SMGs and the SAE in uninjured Lef-$1KI^{+/-}$ mice. However, the finding that MECs of Lef-$1KI^{+/+}$ mice (with two Lef-1KI alleles) spontaneously proliferate and differentiate suggests that this process may be activated by tonic levels of nuclear β-catenin when sufficient Lef-1 is present. Thus, the balance of occupied Lef-1/β-catenin binding sites in the genome, rather than the absolute amount of β-

catenin, maybe be most important to lineage commitment of MECs (Nusse and Clevers, 2017).

While the finding that Lef-1 over-expression enhances the regenerative capacity of multipotent MECs for both SMG and SAE compartments is significant for the field of regenerative medicine, there remain unknown features of this mechanism that require further research. For example, it appears that not all MECs with biallelic Lef-1KI expression ($MEC^{Lef\text{-}1KI^{+/+}}$) are actively replicating in vivo, and while regenerative expansion occurs, it is not indefinite and appears self-limiting. One explanation for these findings could be that available Wnt signals weaken as MEC-daughter cells exit the glandular SC niche. Thus, as $MEC^{Lef\text{-}1KI^{+/+}}$ SCs differentiate into other cell types of the SMGs and SAE, Lef-1 in MEC daughters may no longer have a functional impact. In support of this hypothesis, overexpressing Lef-1 under a club cell-specific promoter (Scgb1a1/CC10) in transgenic mice, or in human tracheal xenografts using viral vectors, had no impact on airway biology (Duan et al., 1999). By contrast, our in vitro culture studies were performed under conditions that promote Wnt signaling (i.e., Wnt agonists) and as such the enhanced proliferative and migratory capacity of $MEC^{Lef\text{-}1KI^{+/+}}$ would be retained. However, the impact of other culture components (i.e., inhibitors of TGFβ/BMP/SMAD signaling) on Lef-1 function remains to be determined.

A second explanation for limited proliferative expansion of $MEC^{Lef\text{-}1KI^{+/+}}$ daughter cells in vivo could be that Lef-$1KI^{+/+}$ overexpression induces symmetric division of MECs to two differentiated daughter cells and/or directed differentiation in the absence of replication. In support of these hypotheses, repeated severe injury of induced Lef-$1KI^{+/+}$ mice clearly demonstrates repopulation of the SAE and SMGs with untraced ($GFP^{+}Lef\text{-}1^{-}$) cells. Thus, high-level unregulated Lef-1 expression in MECs reduces self-renewal of the SC state. Given that Lef-$1KI^{+/-}$ MECs do not spontaneously engage a regenerative response in the absence of injury, the level and/or activity of Lef-1 is likely highly regulated in MECs during lineage commitment. For example, the partitioning of Lef-1-bound DNA to daughter cells could be critical for MEC self-renewing and maintenance of an undifferentiated SC state. Further research is needed in this area.

Taken together, our results demonstrate that glandular MECs are multipotent reserve SCs of both the SAE and SMGs. Induction of Lef-1-mediated Wnt/β-catenin signaling plays an integral role in lineage commitment of MECs and maturation toward SAE basal SCs. Further studies on the MEC SC population identified here will provide greater clarity on transcriptional and environmental signals that control fate decisions in the context of severe airway injury. Such studies are likely to yield important and broadly relevant information regarding epithelial tissue plasticity, in both normal and disease states. Furthermore, the reserve glandular SC compartment may have a more significant role in airway regeneration in humans since SMGs are present throughout the cartilaginous airways, unlike mice.

STAR Methods

CONTACT FOR REAGENT AND RESOURCE SHARING

Further information and requests for resources and reagents should be directed to and will be fulfilled by the Lead Contact, Dr. John F. Engelhardt (john-engelhardt@uiowa.edu).

EXPERIMENTAL MODEL AND SUBJECT DETAILS

Animal Studies—All procedures involving animals were performed in compliance with the protocol (#7031021) approved by the Institutional Animal Care and Use Committee of the University of Iowa and under institutional assurances including: AAALACi accreditation (#000833, since November 1994), USDA research facility registration (USDA No. 42-R-0004), and PHS Animal Welfare Assurance approval (D16-00009, A3021-01). Animals were maintained on a 12 h light/dark cycle and provided with food and water *ad libitum* in individually ventilated units in the specific-pathogen free facilities at the University of Iowa. Female (6 week- to 1.5 year-old) and male (6 week- to 6 month-old) mice of the following genotypes and strains were used: C57BL/6 (The Jackson Laboratory, stock number 000664), B6.129(Cg)-Gt(ROSA)26Sor$^{tm4(ACTB-tdTomato,-EGFP)Luo}$/J x (ROSA-TG) Cre-reporter mice (The Jackson Laboratory, stock number 007676), *MYH11*-Cre^{ERT2} (The Jackson Laboratory, stock number 019079), *ACTA2*-Cre^{ERT2} (generously provided by Dr. B. Paul Herring's lab and maintained on a C57BL/6 background), and ROSA26-CAG-^{LoxP}EGFP^{StopLoxP}Lef-1 mice (maintained on a C57BL/6 background). *ACTA2*-Cre^{ERT2} mice were described previously (Wendling et al., 2009). ROSA26-CAG-^{LoxP}EGFP^{StopLoxP}Lef-1 knock-in mice were used to over express the human *LEF1* transgene in response to Cre and were described previously (Sun et al., 2016). For the purposes of this manuscript, this line is called Lef-1KI. In all studies both male and female mice were utilized with the exception that only male *MYH11*-Cre^{ERT2}:ROSA-TG mice were evaluated, since the *MYH11-Cre^{ERT2}* transgene is on the Y-chromosome. Animals were genotyped at weaning from tail clippings and identified using earhole punches. Experiments were initiated using mice that had no known health/immune concerns, were not involved in previous procedures, and were otherwise drug/test naïve. For lineage tracing experiments Cre-mediated recombination was induced in mice by i.p. injection of 75 μg tamoxifen per gram bodyweight every 24 hrs for a total of 5 consecutive days. Mice were allowed to recover for 5 or 21 days between tamoxifen treatment and injury. Mice were induced with tamoxifen between 6–8 weeks of age. For naphthalene injury experiments mice were injured with a single i.p. injection of either 200 mg/kg or 300 mg/kg naphthalene. Double injury experiments were performed as specified in the figure legends and text and were typically separated by a 21-day recovery period. For SO_2 injury experiments, mice were exposed to 600 ppm SO_2 under atmospheric pressure for 4 hours. A summary of the conditions used for various mouse experiments can be found in the methods Table S4 in the supplemental information.

Culture conditions for in vitro systems—Primary cells were cultured in Small Airway Epithelial Cell Growth Medium (SAGM) (Lonza, Cat#CC-3118) modified with the addition of 10 μM Y-27632 (Tocris, Cat#1254), 1 μM DMH-1 (Tocris, Cat#4126), 1 μM A83-01 (Tocris, Cat#2939), and 1 μM CHIR 99021 (Tocris, Cat#4423) on tissue culture plastic pre-

treated with filter-sterilized laminin-enriched 804G-conditioned media as previously described (Mou et al., 2016).

METHOD DETAILS

Tissue Processing and Cell Isolation—Epithelia from resected mouse tracheae were isolated using a sequential enzymatic digestion strategy as previously described with slight modifications (Lynch et al., 2016). Tracheae were opened longitudinally to expose the SAE and then digested in 1.5 mg/ml Pronase (Roche) in DMEM:F12 at 37°C for 60 minutes with gentle nutation. Tissues were gently agitated to remove SAE and then passed through a 100 μm cell strainer. The flow through containing SAE cells was changed into DMEM:F12 and then into modified SAGM (Lonza) (Mou et al., 2016) prior to plating for culture. The remaining tracheal tissue was then dissected with fine tip surgical scissors into tissue pieces ≤ $3mm^3$ and further digested to isolate SMG cells after washing tissue fragments to remove lightly adherent cells (5 changes of DMEM:F12 by pipetting up and down using a 5 ml plastic pipette). Tissue fragments were then incubated in 2X Collagenase/Hyaluronidase buffer (Stemcell Technologies) diluted in DMEM:F12 at 37°C for 45 minutes with gentle nutation. Pre-wa rmed 0.25% Trypsin-EDTA (Life Technologies) was then added to the cell mixture to a final concentration of 0.05% Trypsin-EDTA and incubated for an additional 30 minutes at 37°C with gentle nutation. After pipetting up and down using a P1000 pipette, a single cell suspension was obtained by passing the cell mixture through a 100 μm cell strainer. The flow through containing SMG cells was changed into DMEM:F12 and then into modified small airway growth media (SAGM, Lonza) as indicated above prior to plating for culture. All centrifugations were performed at 250 × g for 7 min.

Collection of SAE for downstream isolation of basal, club and ciliated cell populations was done as previously described (Zhao et al., 2014). Mouse tracheae were resected and separated from the proximal, SMG-containing portion of the airway and minced. Fragments were incubated in a dissociation solution containing Papain (20U/mL), EDTA (1.1 mM), 2-Mercaptoethanol (0.067 mM), Cysteine-HCl (5.5 mM) and DNAse I (100 U/mL) for 1 hour and 30 minutes. The reaction was stopped with Ovomucoid protease inhibitor (Worthington biochemical Corporation) on a rocker at 4°C for 20 minutes. Cells were then immunostained for FACS analysis as described below prior to resuspending in FACS buffer (2.0% FBS in PBS).

Naphthalene and SO_2 experiments—Adult mice (~8–12 weeks of age) were injured with a single intraperitoneal injection of either 200 μg or 300 μg naphthalene per gram bodyweight. For severe SO_2 injury with 600ppm was administered for 4 hours to adult mice. Mice were hydrated with subcutaneous injections of D5NS (5% dextrose in normal saline) during the first 48 hrs following naphthalene injury. Mock injury was performed with corn oil injection, and served as a baseline control. Mice were allowed to recover following injury (length of time is indicated in each figure legend) before being either re-injured or euthanized for study.

Flow Cytometry—Flow cytometric analysis was performed on cultured primary SAE and SMG cells isolated from *ACTA2*-Cre^{ERT2}:ROSA-TG or *ACTA2*-Cre^{ERT2}:Lef-1KI mice.

Cells were dissociated from plastic plates using Accutase (Stemcell Technologies), changed into HBSS containing 2% FBS, and passed through a 40 μm cell strainer. GFP^+ and $Tomato^+$ (*ACTA2*-Cre^{ERT2}:ROSA-TG mice) or GFP^+ and GFP^- (*ACTA2*-Cre^{ERT2}:Lef-1KI mice) cell populations were identified after gating for viability using Hoechst 33258 (Molecular Probes) at a final concentration of 4 μg/ml. Cells were analyzed and sorted on a FACS Aria II (BD Biosciences). For fractionating SAE into basal, club, and ciliated populations, cells were stained with EpCAM-PECy7 (eBiosciences), GSIβ4-FITC (Sigma), SSEA1-Alexa Fluor® 647 (BioLegend), and CD24-PE (BD Pharmingen) for 30 minutes on ice as previously described (Zhao et al., 2014), prior to FACS. Basal cells were considered EpCAM+ and GSIβ4+. Secretory cells were considered EpCAM+ and SSEA1+. Ciliated cells were considered EpCAM+, GSIβ4- and CD24+. Cell populations were sorted directly into TRIzol (ThermoFisher Scientific) for mRNA isolation.

Competitive Cell Growth Assay—Primary cells from *ACTA2*-Cre^{ERT2}:ROSA-TG, *ACTA2*-Cre^{ERT2}:Lef-$1KI^{+/+}$, and C57BL/6 mice were recovered in modified SAGM (Lonza) as described above. At the time of passage total cells were counted using a Countess Automated Cell Counter (Invitrogen), and 1×10^5 cells were seeded into one well of a freshly prepared 6-well dish. The remaining cells were analyzed with a BD LSR II flow cytometer (BD Biosciences) to determine the percentage of $Tomato^+$, GFP^+, and/or non-fluorescent cells. For reproportioned population mixing experiments, passage 1 (P1) cells were analyzed and sorted on a FACS Aria II (BD Biosciences) into $Tomato^+$ and GFP^+ (*ACTA2*-Cre^{ERT2}:ROSA-TG mice) or GFP^+ and GFP^- (*ACTA2*-Cre^{ERT2}:Lef-$1KI^{+/+}$ mice) populations. Each population was expanded separately to 80% confluence of a 6-well dish as P2 cultures. Competitive cell growth assays were established with 1×10^5 total cells at P3 by mixing $Tomato^+$ or GFP^+ glandular progenitors with non-fluorescent SAE progenitors at a % ratio 10:90 ($SMG^{Tomato+\text{ or }GFP+}$:SAE). To compare wild type MECs (MEC^{WT}) with Lef-1-overexpressing MECs ($MEC^{Lef\text{-}1KI}$), competitive cell growth assays were established by mixing GFP^+ cells isolated from *ACTA2*-Cre^{ERT2}:ROSA-TG mice (MEC^{WT}) with GFP^- cells isolated from *ACTA2*-Cre^{ERT2}:Lef-$1KI^{+/+}$ mice (MEC^{LEF1KI}) at a % ratio of 10:90. All cultures were expanded to near confluency before passaging and quantification of populations.

Migration Assay—Primary MEC^{WT} (GFP^+ cells isolated from *ACTA2*-Cre^{ERT2}:ROSA-TG mice) and $MEC^{Lef\text{-}1KI}$ (GFP^- cells isolated from *ACTA2*-Cre^{ERT2}:Lef-$1KI^{+/+}$ mice) were plated separately at 1×10^5 cells per well on a 6-well dish. Cells were grown as described above. Living cell nuclei were labeled with NucRed Live 647 ReadyProbes Reagent (Invitrogen) by incubating the cells with two drops of reagent per milliliter of media for 30 minutes, and prior to imaging the media was replaced with fresh modified SAGM. Starting eight hours after seeding, live-cell mobility was recorded using a Leica spinning disk confocal microscope fitted with a CO_2 incubation chamber and 37°C heated stage. Images were collected using differential interference contrast (DIC) and a 630nm wavelength far red laser every five minutes for three hours.

Immunofluorescence—Mouse tracheae were fixed in 4% PFA in PBS for 48 hrs prior to washing in PBS and embedding in OCT frozen blocks. Frozen sections were cut at 10 μm.

Frozen tissue sections were post-fixed in 4% PFA for 20 minutes and rinsed in three changes of PBS. Antigen retrieval using citrate boiling was performed on C57BL/6 mice and *ACTA2*-Cre^{ERT2}:Lef-1KI when staining for nuclear Lef-1, Sox-2, TCF7, and β-catenin antigens (note that this antigen retrieval leads to a more diffuse GFP staining pattern in Lef-1KI mice, but is required to detect nuclear Lef-1 and TCF7). Slides were incubated in blocking buffer containing 20% normal donkey serum, 0.3% Triton X-100, and 1 mM $CaCl_2$ in PBS for 1 hr. The slides were incubated with primary antibody (or a mixture of primary antibodies) in diluent buffer containing 1% normal donkey serum, 0.3% Triton X-100, and 1 mM $CaCl_2$ in PBS overnight at 4°C. Slides were washed in three changes of PBS and incubated with secondary antibody (or a mixture of secondary antibodies) in diluent buffer overnight at 4°C. Fluorescent images were collected with a Zeiss LSM 700 line-scanning confocal microscope (Carl Zeiss, Germany). Nuclei were stained using Hoechst 33342 (Invitrogen) or DAPI (4′, 6-diamidino-2-phenylindole) (Invitrogen). Slides were mounted with ProLong Gold (Invitrogen).

Lectin Staining—To stain for mucous cell types of the SMGs and SAE, slides were stained with biotinylated lectins subsequent to immunostaining and prior to coverslipping. Slides were washed in three changes of PBS, and endogenous avidin and biotin were blocked using an Avidin/Biotin Blocking kit (Vector Laboratories) per the manufacturer instructions. Biotinylated lectins, *Dolichos biflorus* agglutinin (DBA) (Vector Laboratories) or *Ulex europaeus* agglutinin I (UEA-1) (Vector Laboratories), were used at a concentration of 10 μg/ml for 30 mins at room temperature. Slides were washed in three changes of PBS and incubated with Alexa Fluor 647-conjugated Streptavidin (Jackson ImmunoResearch 016-600-084) at a concentration of 2 μg/ml for 30 mins at room temperature.

Air-liquid Interface Cultures—Expanded primary cells were grown at an air-liquid interface (ALI) on 0.33 cm^2 polyester transwell membranes (Corning) that were pre-treated with 804G-conditioned media. Each well was seeded with 2×10^5 cells suspended in modified SAGM media (see above). At 16–24 hrs post-seeding, cultures were moved to an air-liquid interface and maintained with Pneumacult ALI media (Stemcell Technologies) for at least 21 days. Mixed-cell ALI cultures were established using FACS purified MEC^{WT} (GFP$^+$ cells isolated from *ACTA2*-Cre^{ERT2}:ROSA-TG mice) and MEC$^{Lef\text{-}1KI}$ (GFP$^-$ cells isolated from *ACTA2*-Cre^{ERT2}:Lef-1KI$^{+/+}$ mice) P2 populations seeded at a 1:1 ratio.

Tracheal xenografts—The proliferative capacity and multipotency of SMG-derived MECs progenitors and SAE-derived progenitors were evaluated in an *ex vivo* tracheal xenograft model as previously described with slight modifications (Engelhardt et al., 1995). Primary cells were isolated from tracheal SAE of wild type mice and SMG of tamoxifen-induced *ACTA2*-Cre^{ERT2}:ROSA-TG mice and expanded *in vitro* as described above to passage 2 (P2). SMG-derived cells including GFP-expressing cells (lineage-traced MECs) and tdTomato-expressing cells (untraced gland cells) were mixed at a ratio of 1:9 (SMG cells:SAE cells) with wild type SAE-derived cells. Denuded tracheal xenografts were also reconstituted with FACS purified SMG cells isolated from tamoxifen-induced *ACTA2*-Cre^{ERT2}:ROSA-TG (GFP$^+$) and *ACTA2*-Cre^{ERT2}:Lef-KI$^{+/+}$ (GFP$^-$) mice and seeded at a ratio of 1:1 (GFP$^+$ WT MECs:GFP$^-$ Lef-1KI MECs). Two-to-three week old ferret tracheal

xenograft scaffolds were freeze-thawed three times and the lumen was rinsed in MEM to remove dead cells. Tracheae were then seeded with 2×10^6 cells total, ligated to flexible tubing, and transplanted subcutaneously into athymic mice. Xenografts were irrigated 1–2 times a week with F12 media and harvested at 5–6 weeks post-transplant.

RNAseq of culture-expanded MECs—Primary glandular cells were isolated from *ACTA2*-Cre^{ERT2}:ROSA-TG and *ACTA2* -Cre^{ERT2}:Lef-1KI$^{+/+}$ mice after five sequential injections of tamoxifen. Primary cells from three to five mice were pooled for each sample. P1 cells were analyzed and sorted on a FACS Aria II (BD Biosciences) collecting lineage-tagged MECs—GFP$^+$ cells (MEC^{WT}) were isolated from *ACTA2*-Cre^{ERT2}:*ROSA*-TG cultures, and GFP$^-$ cells (MEC$^{Lef\text{-}1KI}$) were isolated from *ACTA2*-Cre^{ERT2}:Lef-1KI$^{+/+}$ cultures. Cells were sorted directly into RNA lysis buffer and RNA was extracted using an RNeasy Plus Mini Kit (Qiagen). Samples were treated with DNase and RNA Integrity Numbers (RIN) were assessed using an Agilent BioAnalyzer 2100. All samples had RIN values >10. Indexed cDNA libraries were constructed using a TruSeq mRNA stranded preparation. Normalized libraries were sequenced using 75bp paired-end reads on a HiSeq 4000 (Illumina).

RNA microarray on FACS isolated surface airway epithelial cells—Freshly harvested SAE cells from mouse trachea were FACS sorted into basal, club, and ciliated populations and collected directly into TRIzol (Invitrogen). Total RNA was extracted following a TRIzol RNA isolation protocol and treated with DNase before being assayed on a GeneChip Mouse Gene 1.0 ST Array (Affymetrix).

QUANTIFICATION AND STATISTICAL ANALYSIS

Image analysis—For quantification of tile-scanned fluorescent images, multiple fluorescent channels were quantified using MetaMorph Software's Multi Wavelength Cell Scoring Application Module per manufacturer's instructions. Typically, three sections separated by at least 60 μm were analyzed for each animal, and the average values for each animal were used to calculate the mean ± SEM for each group. Unless otherwise stated, quantification was performed in the C0–C4 region of the trachea from tiled scanned longitudinal images.

Cell Migration Analysis—For each genotype (*ACTA2*-Cre^{ERT2}:ROSA-TG or *ACTA2*-Cre^{ERT2}:Lef-1KI$^{+/+}$) four separate regions from within three independent wells were imaged every five minutes over three hours. Movies were analyzed using the Multidimensional Motion Analysis application in MetaMorph imaging software. To display cell motility paths on a subset of cells in an unbiased manner and to statistically test the difference between MEC^{WT} (*ACTA2*-Cre^{ERT2}:ROSA-TG) and MEC$^{Lef\text{-}1KI}$ (*ACTA2*-Cre^{ERT2}:Lef-1KI$^{+/+}$) motility, single cells from each movie were selected using an online random number generator.

Analysis of MEC RNAseq Data—The number of transcripts per million was calculated for each RNAseq sample using RSEM (Li and Dewey, 2011) and aligned to the Ensembl's mm10 transcriptome. Genes with a mean expression value greater than three times the

standard deviation of that gene within MEC^{WT} or $MEC^{Lef\text{-}1KI}$ sample groups were selected from the dataset as stably expressed genes. Differential expression was determined in R using Benjamini-Hochberg corrected comparisons between MEC^{WT} and $MEC^{Lef\text{-}1KI}$ sample groups. This gene set was used for all subsequent analysis. Principle components analysis was performed using the prcomp function in R (version 0.99.903). Pathway analysis was performed by Ingenuity Pathway Analysis (QIAGEN Bioinformatics).

Analysis of RNA Microarray Data—Raw array CEL files were pre-processed using the mogene10stprobeset.db function within the biocLite package in R and normalized using the Robust Multi-array Average (RMA) algorithm. Multiple probe values for the same gene were aggregated by max probe value. To obtain the gene list corresponding to genes which captured a large amount of the variance in the dataset, we first performed principal components analysis via the prcomp function in R (version 0.99.903). We then found the gene subset which correlated (Pearson $R \geq 0.9$) with either the first or second principal component vectors. Cell type specific genesets were determined through k-means++ via the kmeanspp function in the LICORS package with R, with k=4. A heatmap display of these genes and groups (Figure S5C) was created using the heatmap.2 function in the gplots library within R.

Statistical Analysis—Statistical and graphical data analyses were performed using Microsoft Excel, Prism 7 (GraphPad), R, and Ingenuity Pathway Analysis (QIAGEN Bioinformatics). Details of specific statistical parameters relevant to figures are reported in the figure legend and in the Results section. For all measurements, three or more biological replicates, and two or more technical replicates were used. Information regarding the number of biological replicates “n” used in each experiment is reported in the relevant figure legend and in the Results section.

DATA AND SOFTWARE AVAILABILITY

Raw expression data reported in this paper have been deposited with the Gene Expression Omnibus Database under the accession number GSE111650.

Supplementary Material

Refer to Web version on PubMed Central for supplementary material.

Acknowledgments

This work was supported by NIH grants DK047967, HL051670, DK054759 (to JFE), the Carver Chair in Molecular Medicine (to JFE), and NIH P30 ES005605 (to PST).

References

Anderson PJ, Lynch TJ, Engelhardt JF. Multipotent Myoepithelial Progenitor Cells Are Born Early during Airway Submucosal Gland Development. Am J Respir Cell Mol Biol. 2017; 56:716–726. [PubMed: 28125268]

Browne G, Sayan AE, Tulchinsky E. ZEB proteins link cell motility with cell cycle control and cell survival in cancer. Cell Cycle. 2010; 9:886–891. [PubMed: 20160487]

Clevers H, Loh KM, Nusse R. Stem cell signaling. An integral program for tissue renewal and regeneration: Wnt signaling and stem cell control. Science. 2014; 346:1248012. [PubMed: 25278615]

Driskell RR, Goodheart M, Neff T, Liu X, Luo M, Moothart C, Sigmund CD, Hosokawa R, Chai Y, Engelhardt JF. Wnt3a regulates Lef-1 expression during airway submucosal gland morphogenesis. Dev Biol. 2007; 305:90–102. [PubMed: 17335794]

Driskell RR, Liu X, Luo M, Filali M, Zhou W, Abbott D, Cheng N, Moothart C, Sigmund CD, Engelhardt JF. Wnt-responsive element controls Lef-1 promoter expression during submucosal gland morphogenesis. Am J Physiol Lung Cell Mol Physiol. 2004; 287:L752–763. [PubMed: 15194563]

Duan D, Yue Y, Zhou W, Labed B, Ritchie TC, Grosschedl R, Engelhardt JF. Submucosal gland development in the airway is controlled by lymphoid enhancer binding factor 1 (LEF1). Development. 1999; 126:4441–4453. [PubMed: 10498680]

Engelhardt JF, Schlossberg H, Yankaskas JR, Dudus L. Progenitor cells of the adult human airway involved in submucosal gland development. Development. 1995; 121:2031–2046. [PubMed: 7635050]

Filali M, Cheng N, Abbott D, Leontiev V, Engelhardt JF. Wnt-3A/beta-catenin signaling induces transcription from the LEF-1 promoter. J Biol Chem. 2002; 277:33398–33410. [PubMed: 12052822]

Ghosh M, Helm KM, Smith RW, Giordanengo MS, Li B, Shen H, Reynolds SD. A single cell functions as a tissue-specific stem cell and the in vitro niche-forming cell. Am J Respir Cell Mol Biol. 2011; 45:459–469. [PubMed: 21131442]

Giangreco A, Arwert EN, Rosewell IR, Snyder J, Watt FM, Stripp BR. Stem cells are dispensable for lung homeostasis but restore airways after injury. Proc Natl Acad Sci U S A. 2009; 106:9286–9291. [PubMed: 19478060]

Hegab AE, Ha VL, Gilbert JL, Zhang KX, Malkoski SP, Chon AT, Darmawan DO, Bisht B, Ooi AT, Pellegrini M, et al. Novel stem/progenitor cell population from murine tracheal submucosal gland ducts with multipotent regenerative potential. Stem Cells. 2011; 29:1283–1293. [PubMed: 21710468]

Hogan BL, Barkauskas CE, Chapman HA, Epstein JA, Jain R, Hsia CC, Niklason L, Calle E, Le A, Randell SH, et al. Repair and regeneration of the respiratory system: complexity, plasticity, and mechanisms of lung stem cell function. Cell Stem Cell. 2014; 15:123–138. [PubMed: 25105578]

Lanza, RP., Atala, A. Essentials of stem cell biology. 3. Amsterdam; Boston: Academic Press; 2014.

Li B, Dewey CN. RSEM: accurate transcript quantification from RNA-Seq data with or without a reference genome. BMC Bioinformatics. 2011; 12:323. [PubMed: 21816040]

Liu X, Driskell RR, Engelhardt JF. Airway glandular development and stem cells. Curr Top Dev Biol. 2004; 64:33–56. [PubMed: 15563943]

Liu X, Luo M, Xie W, Wells JM, Goodheart MJ, Engelhardt JF. Sox17 modulates Wnt3A/beta-catenin-mediated transcriptional activation of the Lef-1 promoter. Am J Physiol Lung Cell Mol Physiol. 2010; 299:L694–710. [PubMed: 20802155]

Lynch TJ, Anderson PJ, Xie W, Crooke AK, Liu X, Tyler SR, Luo M, Kusner DM, Zhang Y, Neff T, et al. Wnt Signaling Regulates Airway Epithelial Stem Cells in Adult Murine Submucosal Glands. Stem Cells. 2016; 34:2758–2771. [PubMed: 27341073]

Lynch TJ, Engelhardt JF. Progenitor cells in proximal airway epithelial development and regeneration. J Cell Biochem. 2014; 115:1637–1645. [PubMed: 24818588]

Mou H, Vinarsky V, Tata PR, Brazauskas K, Choi SH, Crooke AK, Zhang B, Solomon GM, Turner B, Bihler H, et al. Dual SMAD Signaling Inhibition Enables Long-Term Expansion of Diverse Epithelial Basal Cells. Cell Stem Cell. 2016

Nikolic MZ, Caritg O, Jeng Q, Johnson JA, Sun D, Howell KJ, Brady JL, Laresgoiti U, Allen G, Butler R, et al. Human embryonic lung epithelial tips are multipotent progenitors that can be expanded in vitro as long-term self-renewing organoids. Elife. 2017; 6

Nusse R, Clevers H. Wnt/beta-Catenin Signaling, Disease, and Emerging Therapeutic Modalities. Cell. 2017; 169:985–999. [PubMed: 28575679]

Pardo-Saganta A, Law BM, Gonzalez-Celeiro M, Vinarsky V, Rajagopal J. Ciliated cells of pseudostratified airway epithelium do not become mucous cells after ovalbumin challenge. Am J Respir Cell Mol Biol. 2013; 48:364–373. [PubMed: 23239495]

Prater MD, Petit V, Alasdair Russell I, Giraddi RR, Shehata M, Menon S, Schulte R, Kalajzic I, Rath N, Olson MF, et al. Mammary stem cells have myoepithelial cell properties. Nat Cell Biol. 2014; 16:942–950. 941–947. [PubMed: 25173976]

Rajagopal J, Stanger BZ. Plasticity in the Adult: How Should the Waddington Diagram Be Applied to Regenerating Tissues? Dev Cell. 2016; 36:133–137. [PubMed: 26812013]

Rios AC, Fu NY, Cursons J, Lindeman GJ, Visvader JE. The complexities and caveats of lineage tracing in the mammary gland. Breast Cancer Res. 2016; 18:116. [PubMed: 27887631]

Rios AC, Fu NY, Lindeman GJ, Visvader JE. In situ identification of bipotent stem cells in the mammary gland. Nature. 2014; 506:322–327. [PubMed: 24463516]

Sun Z, Yu W, Sanz Navarro M, Sweat M, Eliason S, Sharp T, Liu H, Seidel K, Zhang L, Moreno M, et al. Sox2 and Lef-1 interact with Pitx2 to regulate incisor development and stem cell renewal. Development. 2016; 143:4115–4126. [PubMed: 27660324]

Tadokoro T, Gao X, Hong CC, Hotten D, Hogan BL. BMP signaling and cellular dynamics during regeneration of airway epithelium from basal progenitors. Development. 2016; 143:764–773. [PubMed: 26811382]

Tata PR, Rajagopal J. Plasticity in the lung: making and breaking cell identity. Development. 2017; 144:755–766. [PubMed: 28246210]

Teng Y, Li X. The roles of HLH transcription factors in epithelial mesenchymal transition and multiple molecular mechanisms. Clin Exp Metastasis. 2014; 31:367–377. [PubMed: 24158354]

Tetteh PW, Farin HF, Clevers H. Plasticity within stem cell hierarchies in mammalian epithelia. Trends Cell Biol. 2015; 25:100–108. [PubMed: 25308311]

Van Keymeulen A, Rocha AS, Ousset M, Beck B, Bouvencourt G, Rock J, Sharma N, Dekoninck S, Blanpain C. Distinct stem cells contribute to mammary gland development and maintenance. Nature. 2011; 479:189–193. [PubMed: 21983963]

Wendling O, Bornert JM, Chambon P, Metzger D. Efficient temporally-controlled targeted mutagenesis in smooth muscle cells of the adult mouse. Genesis. 2009; 47:14–18. [PubMed: 18942088]

Xie T, Liang J, Liu N, Huan C, Zhang Y, Liu W, Kumar M, Xiao R, D'Armiento J, Metzger D, et al. Transcription factor TBX4 regulates myofibroblast accumulation and lung fibrosis. J Clin Invest. 2016; 126:3063–3079. [PubMed: 27400124]

Xie W, Fisher JT, Lynch TJ, Luo M, Evans TI, Neff TL, Zhou W, Zhang Y, Ou Y, Bunnett NW, et al. CGRP induction in cystic fibrosis airways alters the submucosal gland progenitor cell niche in mice. J Clin Invest. 2011; 121:3144–3158. [PubMed: 21765217]

Xie W, Lynch TJ, Liu X, Tyler SR, Yu S, Zhou X, Luo M, Kusner DM, Sun X, Yi Y, et al. Sox2 modulates Lef-1 expression during airway submucosal gland development. Am J Physiol Lung Cell Mol Physiol. 2014; 306:L645–660. [PubMed: 24487391]

Zacharias WJ, Frank DB, Zepp JA, Morley MP, Alkhaleel FA, Kong J, Zhou S, Cantu E, Morrisey EE. Regeneration of the lung alveolus by an evolutionarily conserved epithelial progenitor. Nature. 2018; 555:251–255. [PubMed: 29489752]

Zhao R, Fallon TR, Saladi SV, Pardo-Saganta A, Villoria J, Mou H, Vinarsky V, Gonzalez-Celeiro M, Nunna N, Hariri LP, et al. Yap tunes airway epithelial size and architecture by regulating the identity, maintenance, and self-renewal of stem cells. Dev Cell. 2014; 30:151–165. [PubMed: 25043474]

Highlights

- Myoepithelial cells (MECs) are reserve stem cells for the surface airway epithelium
- MECs are multipotent and can lineage commit into seven different cell types
- MEC-progenitors can establish SAE residence with lasting regenerative capacity
- Lef-1 overexpression in MECs is sufficient to induce a regenerative response

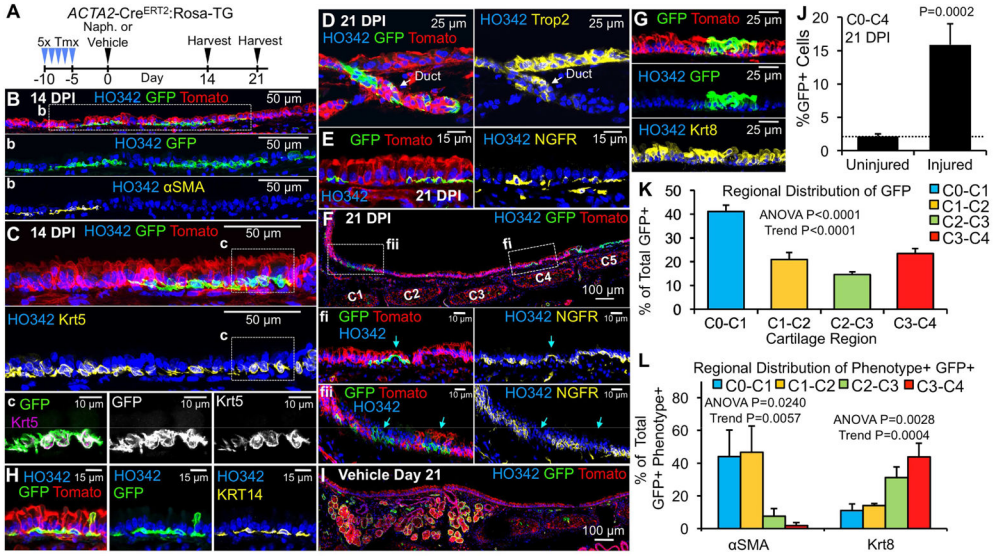

Figure 1. MEC-derived cells emerge from SMGs and adopt a basal cell-like phenotype in the SAE following injury

(A) Timeline of lineage-tracing of myoepithelial cells with tamoxifen (Tmx) and airway injury with naphthalene (Naph). *ACTA2*-Cre^{ERT2}:ROSA-TG mice were treated with tamoxifen daily for 5 days, rested for five days, and then treated with either vehicle or naphthalene (300mg/kg) and euthanized 14 or 21 days post-injury (DPI). **(B–H)** Tracheal sections at the indicated time points are oriented with the proximal region to the left and were stained for nuclei, Tomato, GFP, and the indicated phenotypic markers: **(B)** αSMA expression at 14 DPI (**b:** enlarged image of the boxed region shown in **B**); **(C)** Krt5 expression at 14 DPI (**c:** enlarged image of the boxed region in **C**); **(D)** Trop2 expression in a gland duct at 21 DPI; **(E,F)** NGFR expression at 21 DPI **(fi and fii:** enlarged images of the boxed regions shown in **F**); **(G)** Krt8 expression at 21 DPI; **(H)** Krt14 expression at 21 DPI; and **(I)** Control trachea at 21 days post-induction in the absence of epithelial injury. **(J–K)** Quantitation of lineage-traced cells in the SAE at 21 DPI as **(J)** % of total cells that are GFP$^+$ in the C0–C4 region of the SAE, and **(K)** distribution of total GFP$^+$ cells at various cartilage ring segments. Dotted line in **J** marks background level of signal close to the basal lamina in uninjured controls. **(L)** Distribution of total GFP$^+$ αSMA$^+$ and total GFP$^+$ Krt8$^+$ cells at various cartilage ring segments in the SAE as the % of total C0–C4 GFP$^+$ cells expressing each marker at 21 DPI. Graphs show means +/− SEM for N=6 mice. P-values indicate significance of **(J)** unpaired one-tailed Student's t-test, and **(K,L)** one-way ANOVA followed by posttest for linear trend. See supplemental Figures S1–S3.

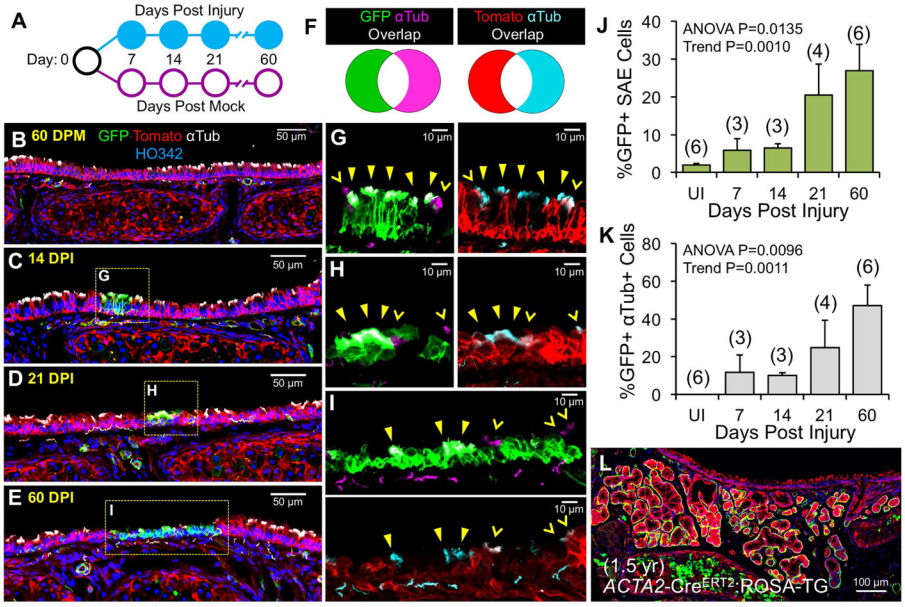

Figure 2. MEC-derived cells produce ciliated cells on the SAE following injury

(A) Experimental design and summary of results: *ACTA2*-Cre^{ERT2}:ROSA-TG mice were induced with tamoxifen as in Figure 1A, treated with vehicle or naphthalene to induce injury, and harvested at the indicated time points. Circles indicate the presence (closed) or absence (open) of lineage-traced ciliated cells on the SAE. Tracheal sections were stained for nuclei, Tomato, GFP, and acetylated αtubulin. **(B)** Vehicle treated mice harvested at 60 days post mock (DPM). **(C–E)** Naphthalene treated mice harvested at 14, 21, or 60 days post injury (DPI). **(F)** Color key for lineage detection of ciliated cells in mice shown in panels **G–I**. The cilia of MEC-derived (GFP$^+$) cells appear either white (left or top panel) or cyan (right or bottom panel); those of cells lacking the lineage-marker GFP (Tomato$^+$) are either magenta (left or top panel) or white (right or bottom panel). **(G–I)** Enlarged, two-channel images of boxed regions in **C–E** show GFP (green)/αtubulin (magenta) and Tomato (red)/αtubulin (cyan). Traced (GFP$^+$) ciliated cells are marked by closed yellow arrowheads, whereas their non-traced (Tomato$^+$) counterparts are marked by open yellow arrowheads. **(J,K)** Quantitation of **(J)** % of total SAE cells that are GFP$^+$ at various DPI and **(K)** % of total GFP$^+$ cells that also express αtubulin at various DPI. Graphs show means +/− SEM for (N) mice as depicted on graphs. (L) Uninjured *ACTA2*-Cre^{ERT2}:ROSA-TG mouse at 1.5 years following tamoxifen-induction. P-values indicate significance of one-way ANOVA followed by posttest for linear trend. See supplemental Figures S1 and S3.

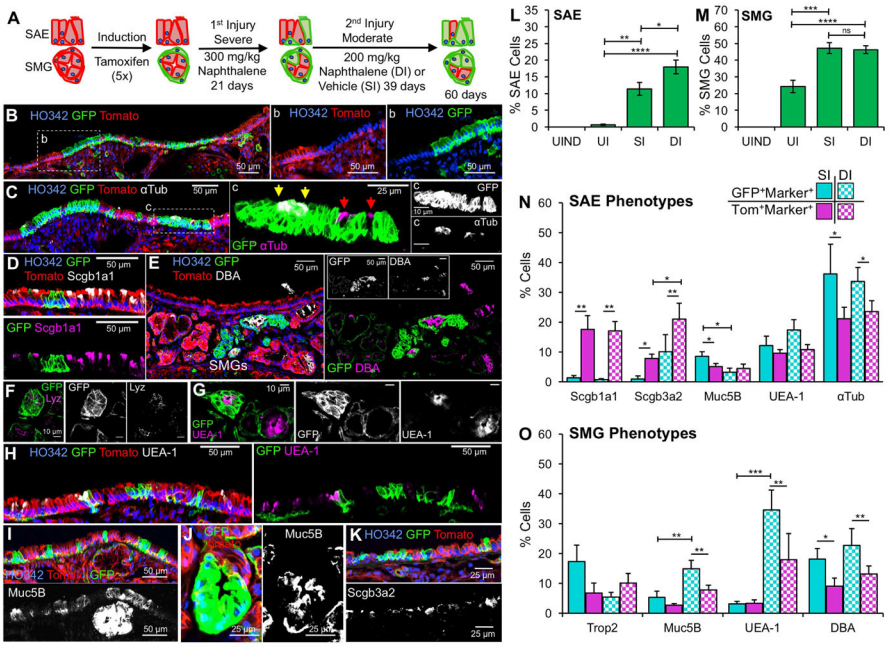

Figure 3. MEC-derived progenitors reestablish niches in the SAE that respond to repetitive injury and are multipotent for both SAE and SMG cell types

(A) Diagram of design for lineage tracing experiment comparing single injury (SI) and double injury (DI). Two other groups of control mice also included: uninduced/uninjured (UIND) and induced/uninjured (UI). **(B–K)** Tracheal sections of DI mice were stained for nuclei, Tomato, GFP, and the indicated phenotypic markers: **(B)** no marker, showing boundary of a lineage-traced group of cells (**b:** enlarged inset from B); **(C)** αtubulin (**c:** enlarged inset from **C**); **(D)** Scgb1a1; **(E)** *Dolichos biflorus* agglutinin (DBA) lectin; **(F)** Lysozyme (Lyz) in SMGs; **(G, H)** *Ulex europaeus* agglutinin I (UEA-1) lectin in **(G)** SMG and **(H)** SAE; **(I,J)** Muc5B in **(I)** SAE and **(J)** SMG; and **(K)** Scgb3a2. Arrows in **c** indicate ciliated cells that are GFP^+ (yellow) or GFP^- (red). **(L,M)** Quantification of the % of total SAE cells that are GFP^+ cells in the **(L)** SAE and **(M)** SMGs for all four groups of mice evaluated**. (N,O)** Quantitation of the **(N)** SAE and **(O)** SMG compartments showing the % of the total GFP^+ cells (cyan) or % of the total $Tomato^+$ cells (magenta) that also express the indicated phenotypic markers after single injury (solid bars) or double injury (checkered bars). Graphs show means +/− SEM for N=4–6 mice per group. P-values indicate significance of **(L,M)** one-way ANOVA and **(N,O)** two-way ANOVA followed by Sidak's multiple comparisons test (ns=not significant, *P<0.05, **P<0.01, *** P<0.001, ****P<0.0001). See supplemental Figures S1 and S3.

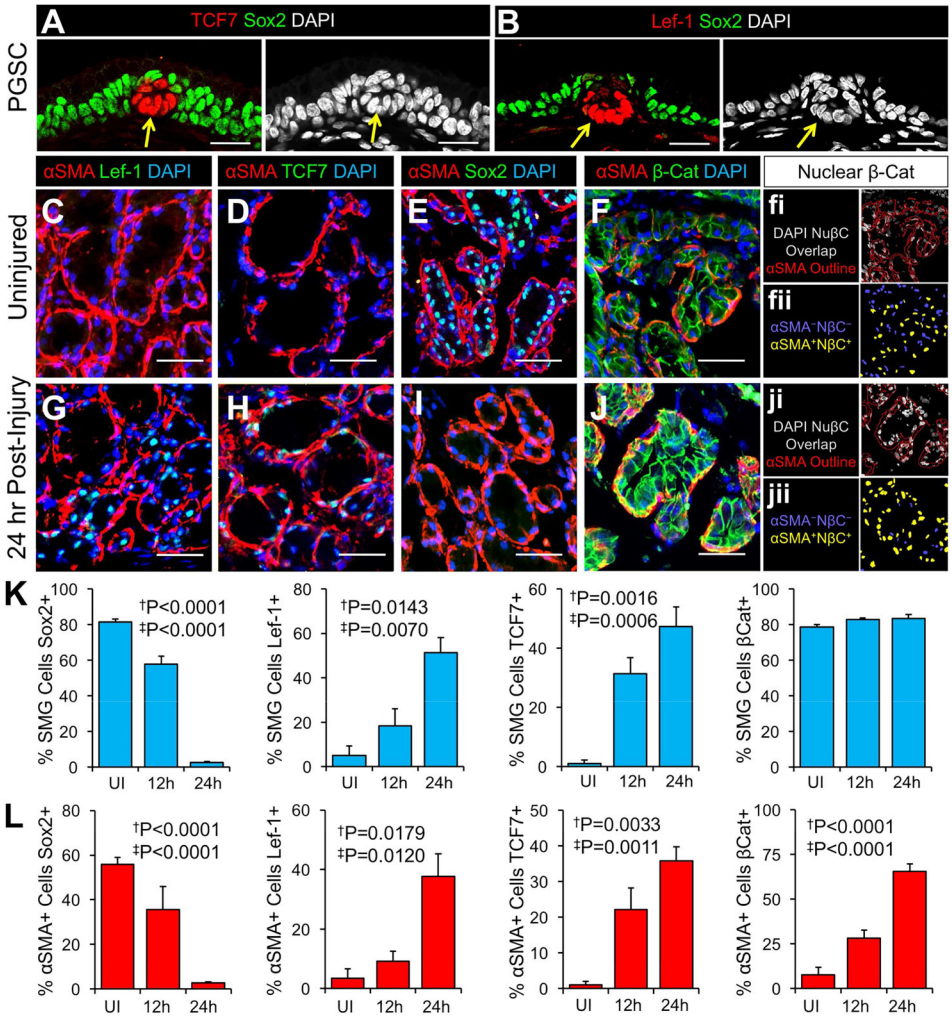

Figure 4. Wnt/β-Catenin signaling is similarly activated in primordial gland stem cells during development and MECs following airway injury

(A,B) Glandular placodes (arrows) from newborn trachea localizing **(A)** TCF7 and **(B)** Lef-1 with Sox2. **(C–J)** Localization of αSMA with Sox2, Lef-1, TCF7, or β-Catenin in SMGs of **(C–F)** uninjured and **(G–J)** 24 hr post naphthalene (300mg/kg) injury. Panels to the right of F and J show **(fi, ji)** nuclear β-catenin (NβC) staining overlapping with DAPI (intensity of β-catenin staining is retained) and superimposed over an outline of αSMA staining (red lines) and **(fii, jii)** representative segmented images after multiwavelength cell scoring each nuclei showing $\alpha SMA^{-}N\beta C^{-}$ (blue) and $\alpha SMA^{+}N\beta C^{+}$ (yellow) cells. **(K,L)** Quantification of nuclear Sox2, Lef-1, TCF7, or nuclear β-Catenin staining as **(K)** the % of total SMG cells and **(L)** the % of αSMA^{+} MECs. Graphs show means +/− SEM for N=3–6 mice per group. All micron bars = 25 μm. Single daggers indicate significance of one-way ANOVA, and double daggers indicate posttest for linear trend. See supplemental Figure S1.

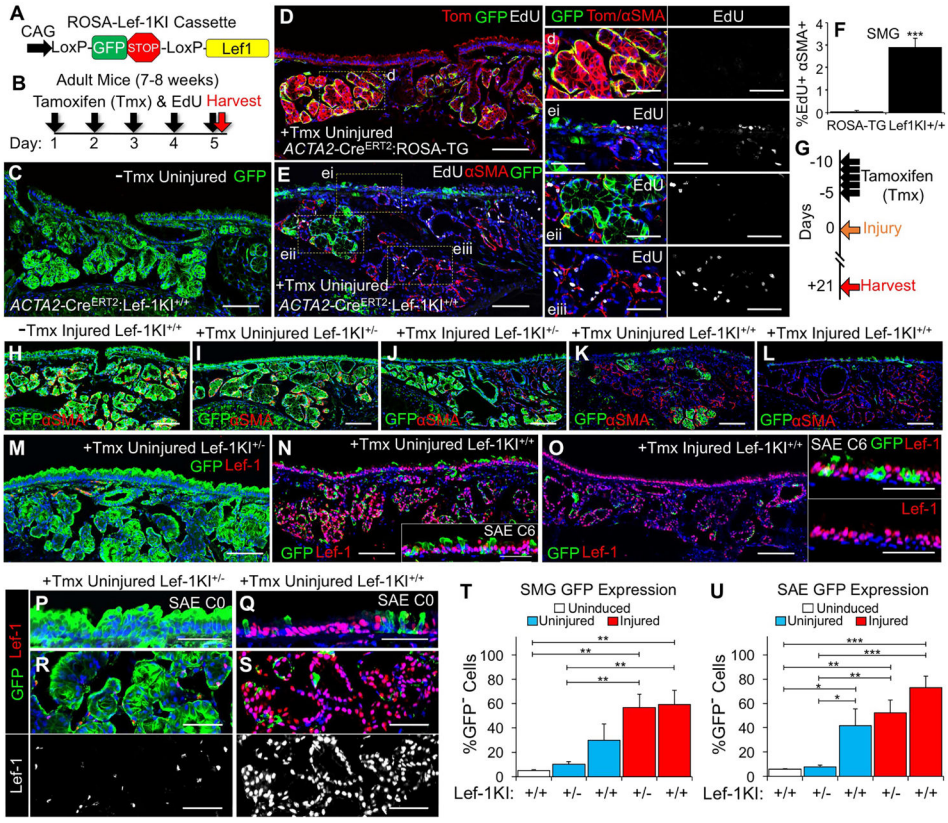

Figure 5. Lef-1 expression activates lineage commitment of MECs and migration to the SAE

(A) Transgenic ROSA26 knock-in construct (Lef-1KI) used to conditionally activate Lef-1 expression in MECs. **(B)** Experimental design for evaluating how Lef-1 expression influences MEC fate in *ACTA2*-Cre^{ERT2}:Lef-1KI$^{+/+}$ vs. *ACTA2*-Cre^{ERT2}:ROSA-TG mice in **(C–F). (C)** Uninduced and uninjured *ACTA2*-Cre^{ERT2}:Lef-1KI$^{+/+}$ demonstrating GFP expression in the majority of cells. **(D,E)** Tamoxifen induced/uninjured mice labeled with EdU as in **(B)** and stained for the indicated markers (d and e**i–eiii:** enlarged insets from **D,E**). **(F)** Quantification of EdU^{+}αSMA^{+} MECs (N=5 mice per group). **(G)** Experimental design for evaluating how Lef-1 dosage impacts MEC fate with and without naphthalene (300mg/kg) injury in **(H–U). (H–S)** *ACTA2*-Cre^{ERT2}:Lef-KI$^{+/-}$ and *ACTA2*-Cre^{ERT2}:Lef-1KI$^{+/+}$ mice were treated under the various conditions as marked and sections stained for **(H–L)** GFP and αSMA or **(M–S)** GFP and Lef-1. Insets of the SAE in **(N,O)** are from different animals at C6. **(T,U)** Quantification of lineage-traced cells (GFP^{-}) as a % of the total cells in the **(T)** SMGs and **(U)** SAE of the C0–C4 tracheal region (N=3–4 mice per group). Graphs show means +/− SEM. Micron bars: (C–E, H–O) 100 μm; (P–S and insets N, O, i–iv) 50 μm. Asterisks indicate significance of **(F)** unpaired two-tailed Student's t-test and **(T,U)** Newman-Keuls multiple comparisons testing (*P<0.05, **P<0.01, *** P<0.001). See supplemental Figure S4.

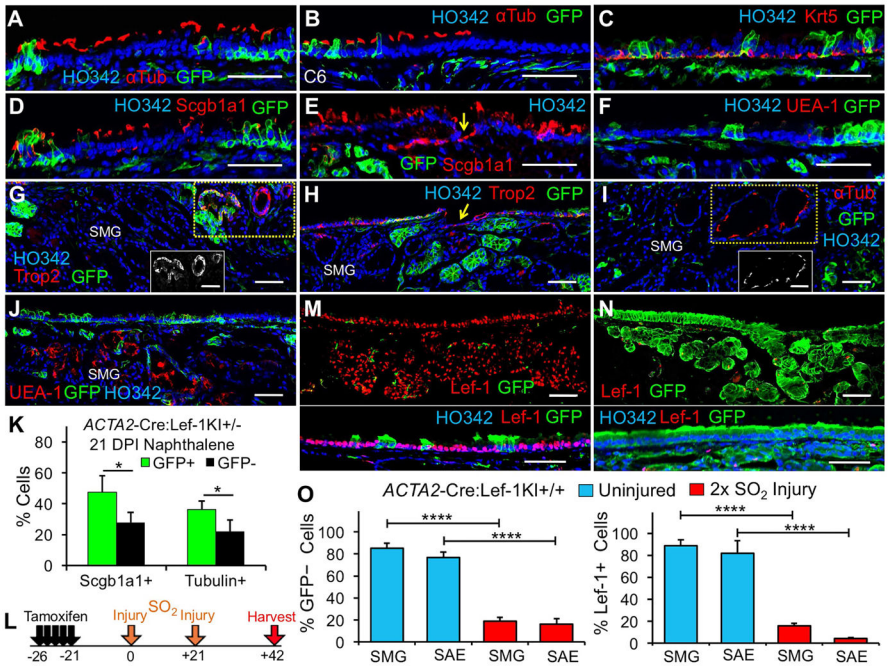

Figure 6. Lef-1 overexpression in MEC SCs promotes terminal differentiation toward multipotent progenitors in the absence of self-renewal

(A–J) *ACTA2*-Cre^{ERT2}:Lef-KI$^{+/-}$ mice were subjected to the injury protocol in Figure 5G and tracheal sections immunostained for the indicated antigens (B&W inset of boxed regions in **G** and **I** show a Trop2^{+} SMG duct and αtubulin^{+} ciliated ducts, respectively). Arrows mark duct openings at the SAE. All images are from the C0–C4 region, except for **(B)** which is at C6. **(K)** Quantification of lineage-traced (GFP^{-}) and untraced (GFP^{+}) club and ciliated cells as a % of total cells in the SAE (C0–C4) from experiments in **(A–J). (L)** Experimental design for evaluating how Lef-1 expression in *ACTA2*-Cre^{ERT2}:Lef-KI$^{+/+}$ mice impacts self-renewal of MECs following sequential SO_2 (600 ppm) injury in **(M,N,O). (M,N)** GFP and Lef-1 immunostaining of tracheas from two **(M)** induced/uninjured and **(N)** induced/2x SO_2 injured *ACTA2*-Cre^{ERT2}:Lef-KI$^{+/+}$ mice. **(O)** Quantification of GFP^{-} and Lef-1^{+} cells as a % of total cells in the SAE and SMGs from experiments outlined in **(L)**. Graphs show means +/− SEM for N=5 mice in **(K)** and N=3 mice per group in **(O)**. Micron bars: 50 μm. Asterisks indicate significance of **(K)** paired two-tailed Student's t-tests and **(O)** two-way ANOVA followed by Sidak's multiple comparisons test (*P<0.05 and ****P<0.0001). See supplemental Figure S4.

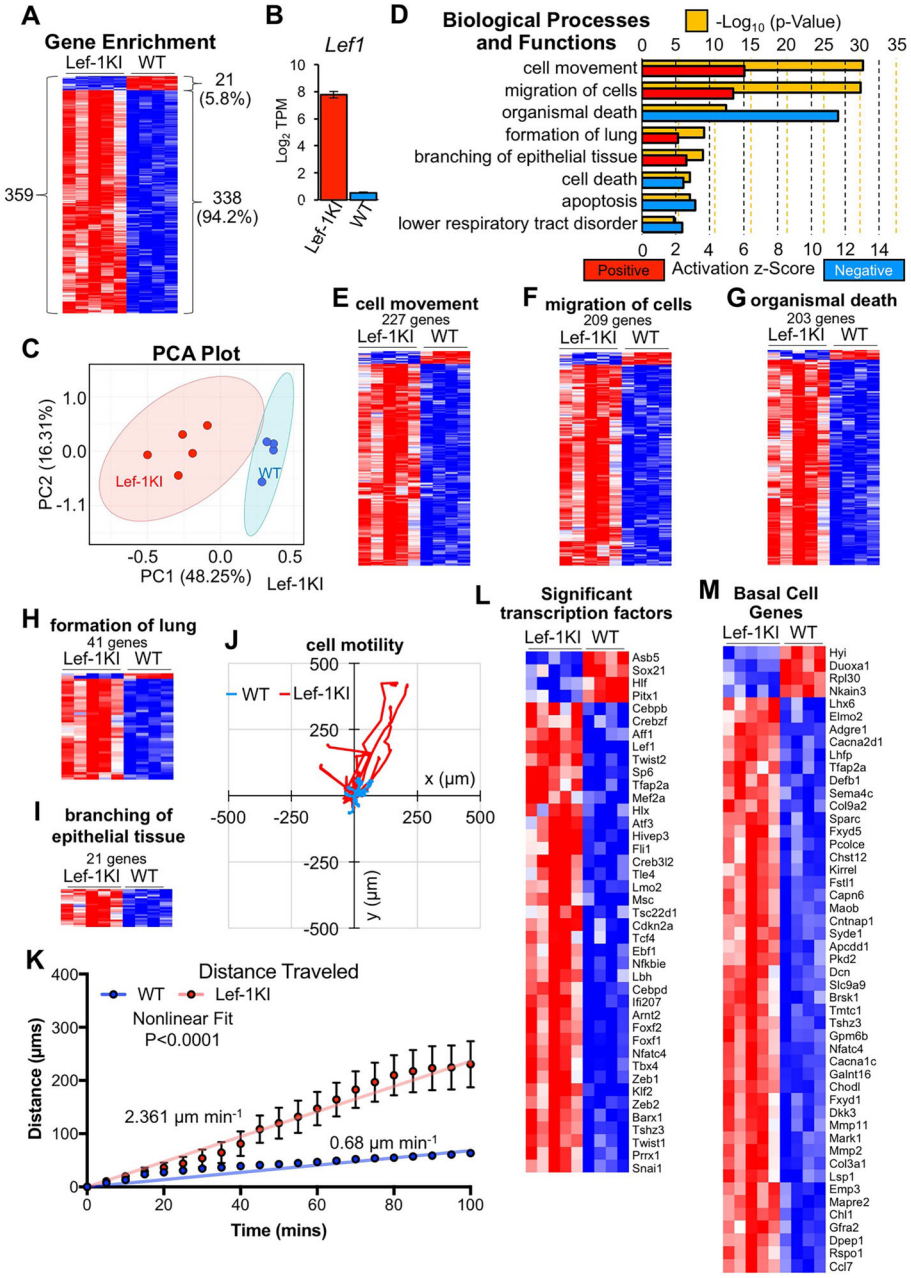

Figure 7. Lef-1 expression in MECs induces regenerative and basal cell transcriptional programs

MECs were isolated from tamoxifen-induced *ACTA2*-Cre^{ERT2}:ROSA-TG (N=4) and *ACTA2*-Cre^{ERT2}:Lef-KI$^{+/+}$ (N=5) mice and purified by FACS at P1 in culture for RNAseq. **(A)** Heat map of 360 differentially expressed genes following unsupervised hierarchical clustering (Benjamini-Hochberg adjusted P<0.05). **(B)** *Lef-1* expression levels in the two genotypes. **(C)** Principle component analysis (PCA) of the 13,337 genes expressed in the two groups. **(D)** IPA biological processes and functions defined by gene expression patterns showing p-values and z-scores. **(E–I)** Heat maps of the indicated IPA gene sets following unsupervised hierarchical clustering. **(J,K)** Motility assays on purified MEC^{WT} and

$MEC^{Lef\text{-}1KI+/+}$ in culture showing **(J)** migration plot and **(K)** distance traveled with time. Measurements were taken of N=16 randomly selected cells traced from N=3 cultures for each genotype from a single experiment; mean +/− SEM is shown in **K** with the P-value indicating the comparison between nonlinear models fitting MEC^{WT} and $MEC^{Lef\text{-}1KI}$ cells. **(L,M)** Heat maps of **(L)** differentially expressed transcription factors and **(M)** basal cell specific genes determined in Figure S5. In all heat maps, red indicates positive enrichment while blue indicates negative enrichment. See supplemental Figures S5–S7 and Tables S1–S3.